Changing Rains Down in Africa: Verifying Shifts in the Position of the Intertropical Convergence Zone Using a New Seasonal Rainfall Model

A Thesis Presented

by

Molly Michael Wieringa

to the

Department of Earth and Planetary Sciences

in partial fulfillment of the requirements

for a degree with honors

of Bachelor of Arts

April 2019

Harvard College

Table of Contents

Abstract

Growing concern surrounding food security in various regions of equatorial Africa has motivated recent efforts to better understand the seasonal precipitation cycle on the continent. Global climate models predict shifts in large-scale drivers of precipitation as a response to anthropogenic climate change; the Intertropical Convergence Zone (ITCZ), a global climate phenomenon connected to equatorial rainfall, is perhaps the most prominent example. While many studies have noted real and present changes in regional seasonal cycles, few have investigated whether such changes might be forced by predicted shifts in large-scale systems. But why should seasonal precipitation be influenced by regional drivers alone? Can evidence for the theorized shifts in the ITCZ be found in the observational rainfall record?

To answer these questions, we propose a novel mixed Gaussian model for seasonal precipitation which isolates metrics for seasonal timing, magnitude, and duration from observational rainfall data. Using these metrics, we track change in seasonal behavior of precipitation over the last century. Trends in seasonal timing across equatorial Africa reinforce the theory of a shifting ITCZ and imply that such a shift has already been initiated. This result underscores the importance of considering both global and regional influences while trying to understand precipitation behavior on any scale. Additionally, changes in seasonal timing will also have very real consequences on agriculture in the region, as the success of rain-fed subsistence crops that feed most of the population depends upon proper timing of planting. As such, understanding changes related to seasonal rainfall may better inform future agricultural practices.

List of Figures

List of Tables

List of Equations

Acknowledgments

This project began as a personal test of whether or not I could carry through with an endeavor as extensive and intricate as a thesis. It has long since become much, much more than an individual journey. The final product is the result of the support, guidance, friendship, and encouragement of a large and amazing group of people.

First, thanks to Peter Huybers, who generously agreed to advise this thesis. From my initial stumbling with Matlab to the refining stages of the final draft, he has been a patient and incredibly knowledgeable touchstone. I am deeply grateful for his constant challenge to see science as more than analysis, to find a question and 'go kick it.' I am likewise grateful for the level of independence he has allowed me to maintain throughout the research and writing process, which has served as the source of the confidence and ability I now feel as a researcher.

Thanks also to Angela Rigden, who so graciously sat through my coding questions and many initial research check-ins. The example and mentorship she provided have made me truly believe I could someday turn my curiosity into a career.

To the entire Huybers research group, thanks for welcoming me, for talking and laughing with me, for checking in throughout the process, and for creating a kind of home within the department.

To my officemates, Becca and Maya, thank you for the months of commiseration, support and late nights eating too much pizza while doing far too little work. I truly would have fallen to pieces without you.

To the Harvard ultimate frisbee community, thank you all for being a place I could go to think about anything other than my thesis, thereby keeping me sane, healthy and happy. Thanks particularly to Will, and to the senior thesis-ers of Quasar, who have obliterated the line between teammates and friends.

To my roommates, thank you for your unconditional love and support, for being the smartest, funniest, and most incredible group of individuals I've ever known, and for not disowning me for disappearing during this last year.

To my father and my sister, thank you for the teasing and poking, and for making me try to be a better person. You are lights in my life, and without you I'd be thoroughly lost.

Finally, as with everything in my life, none of this would have been possible without my mother. Thank you for pushing me more than I could ever push myself and for grounding me more than I could ever ground myself. I love you to the moon and back, a million times.

Introduction

The study of climate dynamics revolves around the idea of balance—the Earth, a closed system, will always seek equilibrium. Any disruption of that equilibrium will be met with a system response intended to achieve a new balance, a restorative feedback on a planetary scale. While such disturbances have occurred many times over the course of planetary history, anthropogenic activity has driven changes 'unprecedented over decades to millennia' (IPCC 2013). The effects fall unevenly on the world's populations (Kotir 2011) and are in most cases still relatively poorly understood on local and regional scales, particularly in Africa, where projected climate change is high and adaptive capacity to change is low (Pereira 2017). Predicted changes in the hydrological cycle of the relatively wet equatorial region are of particular concern to the already water-limited continent, where 85% of people depend upon rain-fed agricultural activities for their livelihood (Kotir 2011). We attempt to better understand and characterize changes in seasonal rainfall by interrogating the implied relationship between seasonal timing and proposed shifts in the first-order drivers of rainfall on the continent, especially those connected to global precipitation systems that are likely to drive change while seeking a new equilibrium (IPCC 2013).

1. Rainfall in Equatorial Africa

The spatial and temporal distribution of Earth's rainfall varies widely according to global, regional, and local controls. Precipitation is concentrated most heavily along the equator, though this distribution varies according to more regional seasonal patterns

(Figure 1). At high latitudes, precipitation forms following the influx of warmer, moister air from the mid-latitudes, which is deposited in the colder polar regions by the global atmospheric circulation, independent of other climate influences. The cooling of deposited air parcels results in lowered saturation mixing ratios, or how effectively air can hold water in the vapor state. Consequently, the moisture in the air parcels is forced to condense and precipitate. At the equator, the characteristic wetness is moderated by a combination of the strong convergence of hemispheric winds and consistent direct solar radiation, which drives uplift of warm, relatively moist air that eventually cools according to the same mechanism, creating a region of high annual precipitation hereafter referred to as the tropical rain belt. The rain belt is well documented and recognizable from space, as nearly all of the planet's rainforests lie in close proximity. Despite its global presence

Global Average Annual Precipitation

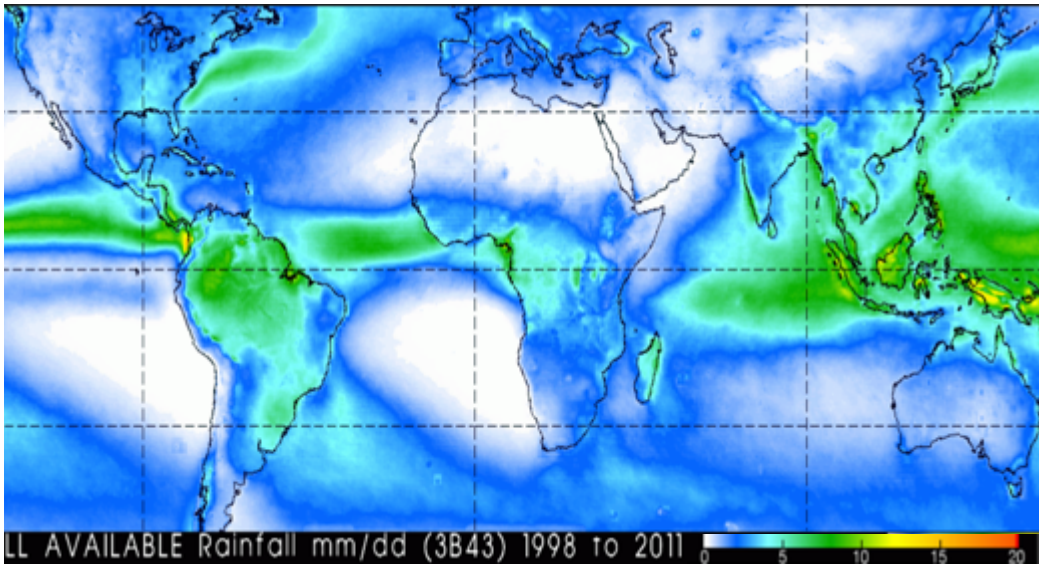

Figure 1: Global rainfall averages from 1998-2010, compiled from TRMM precipitation satellite data (NASA). White and blue colors indicate areas of lesser precipitation, while reds and oranges highlight areas of very high precipitation.

and regulation by large-scale phenomena, the rain belt lacks uniformity—it varies more across continents than oceans worldwide. Across Africa and Africa only, that variability manifests as less rainfall (Figure 1).

The African equatorial region has already been described as a major dry anomaly relative to the rest of the notably wet global equatorial belt (Camberlin 2018), and the Greater Horn of Africa's low-level precipitation pattern in particular has been referred to as "perhaps the most impressive climate anomaly on the continent" (Trewartha 1961). Other areas of interest are the breadbasket Sahel region at the northern extreme of the rain belt, just below the Sahara's southern border, and the Congo River Basin, which receives the highest concentration of rainfall in Africa (Figure 2). Fortunately, the relative dryness of the continent and the contrasts between spatial regions magnify seasonal patterns when compared to the rest of the continental tropics, allowing for a clearer

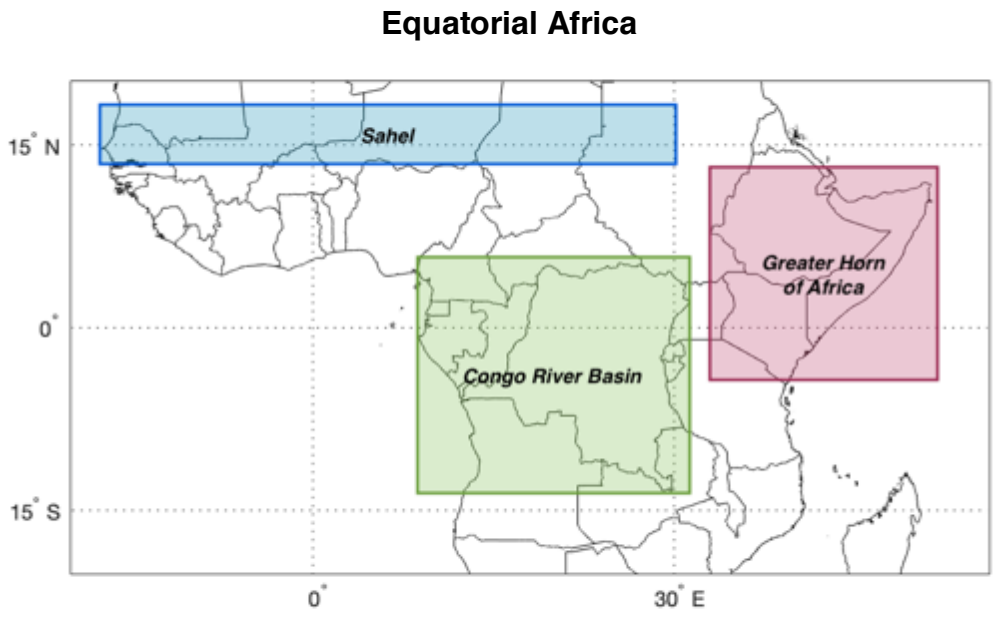

Figure 2: Heavily studied regions of equatorial Africa, where boxes represent the general area in which research has been focused. The Sahel is shown in blue, the Congo River Basin in green, and the Greater Horn of Africa in red.

understanding of the larger picture of annual and historic rainfall in the tropical region of Africa.

2. Seasonality and the Intertropical Convergence Zone

The area of convergence along the global equator is known as the Intertropical Convergence Zone (ITCZ). The ITCZ tracks closely with the earth's thermal equator, which receives the greatest amount of solar insolation. Both the convergence of winds deflected from midlatitudes associated with the ITCZ and the heating caused by direct sunlight at the thermal equator drive the central ascending branches of the global Hadley circulation, a primary modulator of air uplift and equatorial precipitation (Figure 3); as such, the two terms are often used interchangeably in the literature. This synonymy has created an inconsistency of definition—studies describe the ITCZ's characteristics and location relative to the chosen variable of focus, resulting in some confusion regarding its actual physical basis (Nicholson 2018). Recent work has called into question the colocation of the ITCZ and the thermal equator, as well as the directness of their relationship to tropical rainfall. These studies note a physical displacement between the ITCZ as defined by surface pressure and convergence as well as the zone of maximum rainfall (Dezfuli 2017; Nicholson 2018). However, the realization of such a displacement has not successfully discredited the obvious connection between the ITCZ and rainfall location and seasonality. We therefore choose to understand the ITCZ as a heat- and energy-dependent system which exerts a first-order influence on rainfall in the African

equatorial region and proceed to analyze it in relation to measured rainfall, the object of primary concern within this study.

While the ITCZ and its effects on the rain belt are most prevalent in the tropics, the range of seasonal and regional patterns within the tropical region defies characterization in a single analysis. Existing literature recognizes two broad but distinct annual seasonal patterns along the African equatorial band.

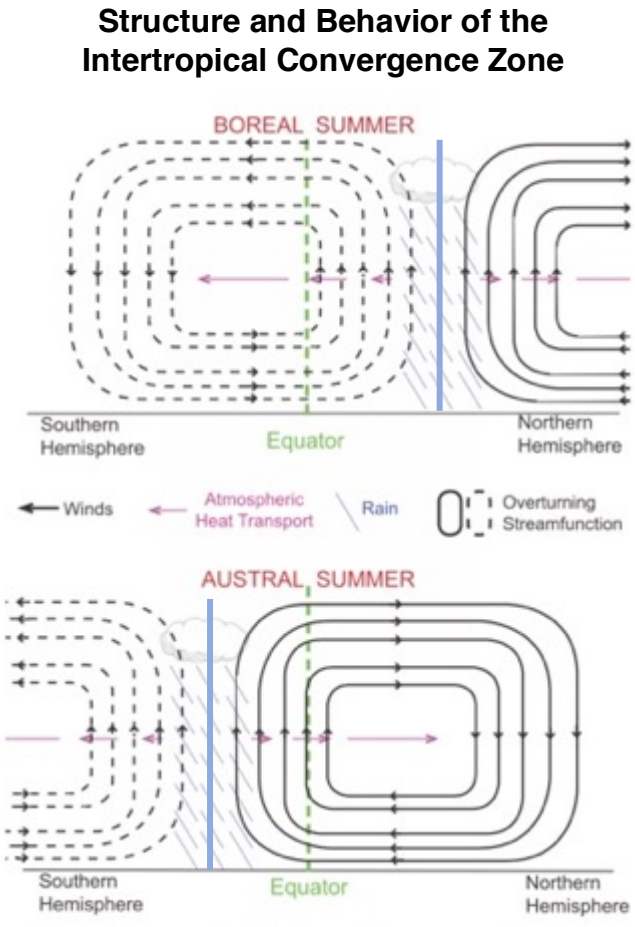

Figure 3: Hadley cell circulation for boreal summer (top) and winter (bottom). Dashed/solid contours represent overturning streamfunction towards and through the southern/northern hemisphere, purple arrows represent atmospheric heat transport, and the solid blue line represents the approximate location of the ITCZ (modified from Donohoe et al. (2012).

The first represents one seasonal cycle—a single annual dry period followed by a single annual wet period. The second annual pattern represents two seasonal cycles—typically boreal spring and fall wet periods, separated by boreal summer and winter dry periods. Whether a region experiences a single or a double rainy season depends upon its location relative to the ITCZ.

In particular, the ITCZ demonstrates a strong control of seasonality along the equator. Because of its connection to the thermal equator, the convergence zone oscillates latitudinally across the equator

throughout the year, 'following' convection driven by solar radiation until the cooler temperatures of the mid-latitudes can no longer support further poleward movement (Figure 4). Once this critical point is reached, the ITCZ begins migrating back toward the equator, all the while pulling the rain belt in its wake. Regions in close proximity to the equator or at the latitudinal extremes of the ITCZ's path, where the ITCZ is present twice a year, generally express the double rainy season pattern. The latitudes in between generally contain some part of the rain belt for the entirety of the ITCZ's traverse through a respective hemisphere, and therefore express a single rainy season. The timing, duration, and magnitude of rainfall in each of these individual seasons varies across the study region.

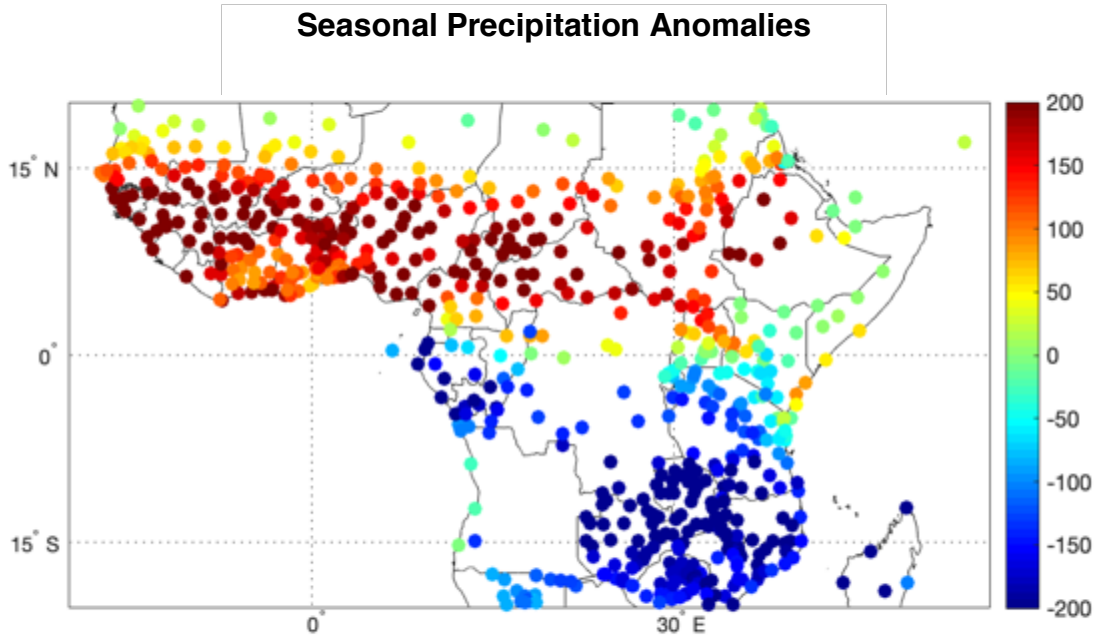

Figure 4: Global seasonal-scale precipitation anomaly, found by subtracting the boreal winter (DJF) precipitation from boreal summer precipitation (JJA). Blue shading indicates the position of the rain belt during the boreal winter, red shading indicates rain belt position during the boreal summer (based on Putnam & Broecker 2017).

3. Literature Review

Plenty of existing studies explore the variation of seasonality across equatorial Africa. The majority of the literature focuses on a particular sub-region, such as the Greater Horn of Africa (Camberlin 2018; Nicholson, 2017; Schreck and Semazzi, 2004; Tierney et al. 2013; Tierney, Ummenhofer, and deMenocal 2015; Tierney and deMenocal 2013; Yang et al. 2015), the Sahel (Schewe and Levermann 2017; Thomas and Nigam 2018), or Western and Central Africa (Dezfuli 2017; Dezfuli and Nicholson 2013; Nicholson and Dezfuli 2013), and has therefore identified mechanisms that drive the spatial variability of seasonality within the broader pattern dictated by the ITCZ and the rain belt.

For example, Yang et. al. (2015) explore the effects of the Asian monsoon on Eastern Africa, which experiences the system's western edges. The monsoon is a complex intersection of seasonally shifting winds and Indian Ocean sea-surface temperature patterns, which helps govern the seasonal cycle in the sub-region. As the monsoonal winds shift the location of their arrival from the northeast in the boreal fall and winter to the southeast in the boreal spring and summer, they ventilate the region by bringing in air from the Indian Ocean and causing increased divergence and precipitation (Figure 5). Western and central equatorial Africa (WCEA) may be secondarily influenced by these dynamics, as the eastern and western halves of the equatorial continent are thought to be connected by a Walker-like recycling circulation pattern that could translate the effects in one region into related effects in the other (Dezfuli 2017) (Figure 6). In addition, seasonally-phased precipitation in WCEA coincides with a secondary area of

low-level convergence known as the Congo Air Boundary, which separates the moist air of the Congo region from the relatively dry, stable air from the monsoons (Dezfuli 2017).

Tierney, Ummenhofer, and deMenocal (2015) draw parallels between past climate changes and the recent decline in boreal spring rainfall in the Greater Horn of Africa (GHA) by delving into a compiled paleoclimate record of precipitation off the

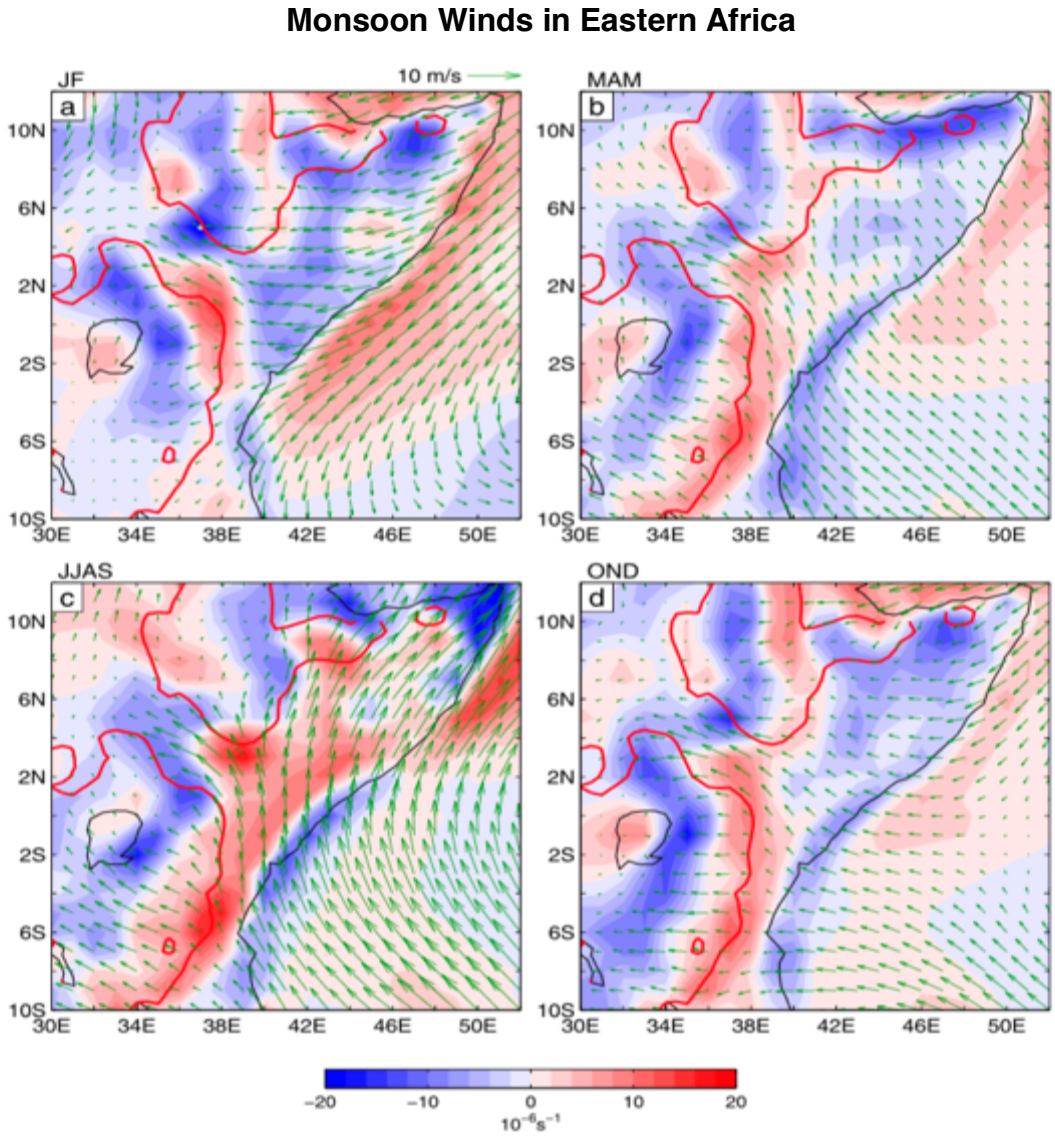

Figure 5: Seasonal climatologies of the 10-m wind vectors and associated divergence (colors, 10-6s-1) from ERA-Interim, illustrating the seasonal ventilation of Eastern equatorial Africa (adapted from Yang et. al. 2015)

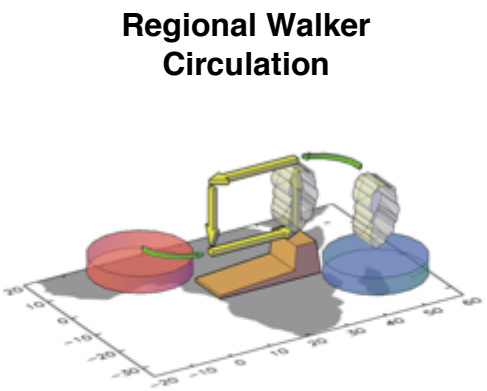

Figure 6: Schematic illustration of key components of the regional Walker circulation across equatorial Africa, also called the zonal asymmetric pattern (ZAP) during a positive phase. Yellow arrows show the zonal atmospheric circulation, red/blue regions indicate positive/negative pressure anomalies, green arrows depict influx and outflow of winds, defected by the Coriolis force (adapted from Dezfuli 2017).

Gulf of Aden. They demonstrate a possible anthropogenic component of the precipitation decline and a mechanistic connection with the Indian Ocean, but also highlight the discrepancy between climate models' predictions for Eastern Africa and those based upon observation data. They ultimately call for 'an accurate simulation of the seasonal cycle' and a better holistic understanding of regional seasonal dynamics (Tierney, Ummenhofer, and deMenocal 2015).

Nicholson and Dezfuli (2013) have written a two-paper analysis of interannual variability in the seasonal cycle across Western and Central Equatorial Africa, focusing the first installment on the boreal spring season and the second on the boreal fall. In the course of the exhaustive study, they explore correlations between precipitation and sea-surface temperature, sea-level pressure, and atmospheric features, such as the Tropical Easterly Jet. Through both papers, they build a comprehensive picture of varied oceanic and atmospheric influences, emphasizing the probable secondary nature of the correlative relationship between precipitation and sea surface temperature (SST). They argue instead that SST reflects shifts in atmospheric pressure that are more likely to be causal mechanisms behind precipitation shifts. Both papers acknowledge that high precipitation

anomalies correlate negatively with SST in the Indian Ocean and the eastern Pacific, and that the intensity of a concurrent season is negatively correlated between the western and eastern equatorial regions.

Other studies have drawn correlations between seasonality and the El Niño Southern Oscillation (ENSO) (Camberlin, Janicot, and Poccard, 2001; Nicholson and Kim 1997; Ropelewski and Halpert 1987), and identified regional connections between seasonality and both Atlantic and Pacific sea surface temperature (Balas, Nicholson, and Klotter 2007; Camberlin 2018; Kazadi and Kaoru 1996). Additionally, factors such as land-use change (e.g. deforestation) and aerosol concentration have been suggested as tertiary controls on precipitation in the region (Chakraborty et al. 2016; Dezfuli 2017).

The importance of regional controls and the influences explored in these studies should not be understated. However, they operate within the pattern regulated by the ITCZ, and efforts to understand change within the region should be predicated on an understanding of the larger system. In the context of anthropogenic climate change, a new literature pertaining to expected deviations of the ITCZ pattern has appeared. Putnam and Broecker (2017) predict a northward shift of the tropical rain belt due to differential heating of the northern and southern hemispheres. Using theories based upon climate models, they argue that the doubly intense heating of the Northern Hemisphere, which contains far more land than the Southern Hemisphere, has altered the energy input of the atmosphere and should pull the ITCZ north relative to its current location (Putnam and Broecker 2017). This prediction is supported by theoretical and empirical work which demonstrates an anti-correlation between the position of the ITCZ and both atmospheric heat transport and cross-equatorial energy flux (Bischoff and Schneider

2014; Donohoe et al. 2012; Frierson and Hwang 2012). In straightforward terms, the more rapid heating of the Northern Hemisphere creates a global energy imbalance; in theory, the imbalance should be corrected as heat transport to the Southern Hemisphere increases in response to a northward shift of ITCZ, allowing the ascending branch of the convergence system to transport more energy across the equator (Figure 3). Shifts of this kind have occurred in the geologic past and in regions other than equatorial Africa: Arbuszewski et al. show that the Atlantic Ocean ITCZ shifted by up to 7 degrees of latitude between the Last Glacial Maximum and the early Holocene (Arbuszewski et al. 2013), and Si et al. relate the northerly shift of East Asian Meiyu rain belt to shifts in the ITCZ and western Pacific subtropical high pressure system (Si, Ding, and Liu 2009). While climate models also predict such behavior, a shift of the ITCZ in the age of anthropogenic climate change has not yet been demonstrated.

Such a shift would undoubtedly impact seasonality of rainfall in equatorial regions and would logically be reflected in seasonality parameters such as timing or magnitude. Few if any previous studies have sought to explicitly link seasonality to a shifting ITCZ, but many have developed methods for quantifying seasonal attributes. Liebmann et. al. (2007) define seasonal timing and duration using “onset” dates calculated by determining sustained anomalous accumulation periods. Seregina et. al. (2019) have likewise derived onset and cessation definitions using pentad averages and climatological reference time series. Feng et. al. (2013) derive a seasonality index, a single number that describes precipitation distribution throughout a calendar year. Many other studies simply use a calendric system, which obtains quantifiable metrics using data within groupings of calendar months. Many of these methods were developed within the

context of a specific study, though Seregina et. al. (2019) attempt to create a widely applicable model. All previous methods rely on some measure of quantity of rainfall, which is subject as much to regional and local influences as to large-scale systems like the ITCZ. After weighing the pros and cons of each of these various methods, we have proposed a similarly flexible yet improved alternative method for quantifying seasonal behavior. Our model's explicit focus on seasonal timing is intended to better reflect the long-term behavior of the ITCZ.

4. Motivation

Africa's primarily tropical position and the limited ability of most African countries to adapt to climate change ensures the continent's place as one most affected by future climate alterations (Pereira 2017). Rising temperatures and shifting precipitation patterns will only further strain the already limited resources of the region, lessening crop yields and water availability (Kotir 2011; Pereira 2017). In addition to increased strain on existing agricultural locations, the continent is projected to lose 18% of its arable land by 2100 (Kotir 2011). The massive ramifications for human populations on the continent and the scientific uncertainty surrounding current projections of its future are our key motivations.

Human Motivation

Rain-fed agriculture comprises 97% of total crop land in sub-Saharan Africa, and only 4% of current production area is irrigated (Kotir 2011). The agricultural system relies almost exclusively on precipitation, and as much on the timing of rainfall as on the total amount. Subsistence crops such as sorghum, millet, and maize are grown widely and

form the basis of much of the population's diet (National Research Council 1996); a shift in the timing of rainfall without a corresponding shift in the timing of planting could be devastating to food security in the equatorial region. Agricultural activity contributes over 25% of GDP on the continent, which includes six of the world's ten fastest growing economies (Pereira 2017), and which must somehow handle a projected population increase of over 1 billion people by 2050 (from 2005 levels) (Kotir 2011).

The impacts of climate change, especially those related to temperature and precipitation, have a singularly catastrophic potential for devastation in Africa. Understanding both recent and future potential changes in rainfall distribution may be crucial in allowing countries to accelerate their ability to adapt, thereby mitigating food insecurity and the toll on human populations.

Scientific Interest

The quest to confront questions related to precipitation faces many difficulties in any region of the world—in Africa, the scarcity, intermittency and unreliability of *in situ* data constitute an additional and often seemingly insurmountable problem. Climate models, which lack the density and continuity of observations required for proper calibration, represent the region poorly, and studies incorporating these models are often at odds with those projects based upon the available observations. We hope to be able to use our seasonal rainfall model to overcome some of the data intermittency that appears to have spatially limited previous studies, thereby more accurately investigating questions related to both regional and continental precipitation change. We expect that our findings will validate theories related to change in large-scale systems such as the ITCZ, while also shedding further light on the complexities of overlaid regional patterns.

5. This Study

In the interest of trying to isolate meaningful shifts in precipitation most likely to impact the lives of those living in equatorial Africa, this thesis focuses on changes in rainfall timing as well as seasonal magnitude and duration, hereafter referred to collectively as seasonality. For the purposes of agricultural stability, these parameters are at least as significant as the more commonly used onset, cessation, and total annual rainfall, as they play a role in dictating the success of seasonal crops. The movement of the ITCZ and the tropical rain belt between hemispheres determines the broad regional-scale precipitation from season to season, and as such is of primary interest when exploring seasonal patterns (Figure 4). We investigate this movement using a new statistical model, and use the results to expand, corroborate or challenge existing theories of continental and regional change in the position of the ITCZ.

.

Methods

1. Data and Study Region

Many studies of rainfall in equatorial Africa have focused separately on characteristic climatic zones such as the Greater Horn of Africa, the Sahel, or Western and Central Africa in order to isolate the varied influences on rainfall patterns in each zone. As we seek to identify and investigate large-scale changes in rainfall seasonality, we have chosen a study region that includes all of the above sub-regions. The area of interest extends from just south of the Tropic of Cancer at 20°N to just north of the Tropic of Capricorn at 20°S and spans the width of the equatorial African continent, from 10°W to 55°E. The region is thus extremely varied with regards to topography, proximity to major bodies of water, land cover, and density of observations. In keeping with the existing literature and for the sake of clarity, much of the analysis performed in this thesis is based first upon the sub-regions, then aligns those individual scientific narratives to form a larger understanding of historical rainfall and the ITCZ across the entire African equator.

Data Criterion

Several types of historical precipitation records exist for equatorial Africa, including but not limited to direct rain gauge measurements, reanalysis products, satellite observations, and modeling exercises. The scarcity and intermittency of direct observational precipitation measurements in the region of interest are well-recognized in related previous studies, but satellite and reanalysis alternatives present equally worrying concerns.

The United States National Aeronautics and Space Administration (NASA) has collaborated on two satellite precipitation measurement missions. The first, the Tropical Rainfall Measuring Mission (TRMM), launched in 1997 in partnership with the Japanese Aerospace Exploration Agency, used microwave imagery to quantify water vapor, cloud water, and precipitation intensity in the atmosphere (NASA 2019). The mission expired in 2015 and was replaced by the Global Precipitation Measurement (GPM) mission, a core microwave radiometry satellite capable of providing a calibration standard for an entire suite of international satellites (NASA 2019). While these measurements are vital to an increased understanding of climate change and global weather patterns, the limited timeframe during which they are available does not allow for a conclusive historical study of seasonal rainfall.

Some historical precipitation studies attempt to circumvent the problem of spatially uneven or temporally inconsistent data using gridded or reanalysis products. However, reanalysis precipitation products, as in the National Centers for Environmental Prediction–National Center for Atmospheric Research (NCEP-NCAR) global reanalysis project, do not generally incorporate precipitation observations; precipitation data is not assimilated into the project's model, and the precipitation product is therefore a set of accumulations based upon 6 – hour forecasts (Janowiak et al. 1998). Janowiak et. al. (1998) demonstrated good agreement over large scales and across annual mean rainfall between NCEP-NCAR and rain gauge-based observational data, but also illustrated poor agreement across regional features and generally low correlations between the two datasets in equatorial land regions. For these reasons, we have chosen to avoid the use of

reanalysis products, despite the uneven spatial and temporal distribution of observational data.

Global Historical Climate Network

The bulk of the data used in the course of this thesis is a subset of the Global Historical Climate Network (GHCN) v.2 dataset, which was published in 1997 and replaced an earlier version released in 1992. The second version addresses a number of concerns related to data availability and quality by adding new sites, assessing data quality, and introducing homogeneity adjustments to reduce the non-climatic side effects of rain-gauge measurement collection (Peterson et al., 1998; Peterson and Vose 1997). While equatorial Africa remains a data-poor region, the network of GHCN sites across the region of interest is sufficiently dense to warrant continued study.

From the original GHCN v.2 dataset, we have selected sites which have had over 50 years of data collected, minimizing to some extent the temporal variability within our

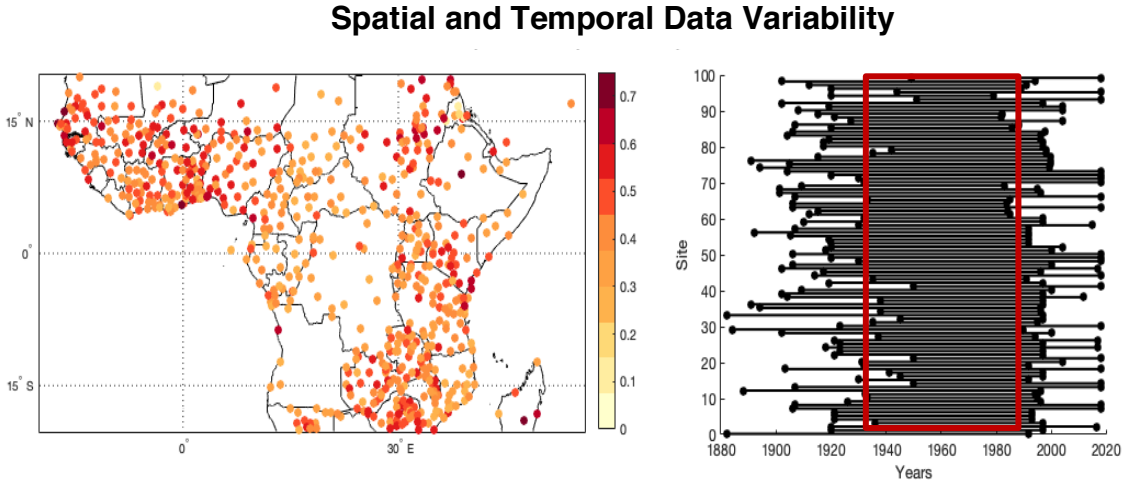

Figure 7: Spatial (left) and temporal (right) variability of GHCN measurements. Spatial variability is represented as a percentage of the entire dataset window (1984-2018) for which measurements at a specific location exist; temporal variability is represented by 100 randomly selected sites from the dataset. The red box outlines the timeframe over which we perform our analysis (1936-1988). During this time, no sites are missing more than 25 percent of data.

data subset, while necessarily increasing the uneven spatial distribution (Figure 7). In particular, though the earliest record included in our data subset is 1848, there are too few observations before 1936 at any site to usefully analyze rainfall behavior prior to the turn of the twentieth century. A less severe though still significant absence of rain gauge data also defines years after 1988. Most of the analysis underlying this project therefore focuses on the mid-twentieth century (1936-1988), using the measurements from 1946-1975 as a climatological mean.

Though our decision to avoid the complications of reanalysis products and the limited range of the satellite record is justifiable, the focus on observational data introduces a number of secondary complications. As will be discussed in later sections, we attempt to mitigate these issues through a combination of statistical modeling and regional clustering.

Tropical Precipitation Measurement Mission

Though the GHCN subset comprises the majority of data analyzed in this study, we have also chosen to incorporate satellite data from the Tropical Precipitation Measurement Mission (TRMM) dataset, available from NASA. GHCN records extending beyond the early 1990s are sparse, and other precipitation missions, like GPM, did not come online until the mid-2010s. TRMM, which officially covers the period 1997– 2015 but incorporates GPM data up to 2017, provides the least disruptive addendum to our chosen GHCN record.

TRMM and GHCN are not directly comparable datasets—TRMM has been shown to miss light rain events (Contractor et al. 2015) and derives precipitation measurements from microwave radiometry as opposed to direct collection. We therefore

exercise caution when drawing conclusions from analyses applied to both TRMM and GHCN.

2. Mixed Gaussian Model

The natural noisiness of rainfall data and the temporal variability of the available data make isolating seasonal characteristics in the region—and any significant related changes therein—quite difficult from data alone. To address the problem of missing data and the need to isolate measures of when, for how long, and how intensely each rainy season arises, we have designed a simple statistical model for annual rainfall, based on Gaussian distributions. When applied, the model's Gaussian variable outputs can be used as reasonable measures of timing, duration, and magnitude for each individual season.

Design and Applicability

While monthly rainfall data are substantially less noisy than daily measurements, using raw data to obtain measures of seasonal timing and duration can still lead to inconsistent or noisy seasonal parameters. Modeling annual cycles of rainfall according to our proposed method presents a convenient alternative that filters out some natural variability. Close examination of rainfall time-series reveals annual distributions that approximate a periodic curve. Due to the relative independence of the boreal spring and boreal fall seasons in the double-cycle sites, this curve is not quite sinusoidal. In order to capture the individual timing, duration and intensity of each individual season, we chose instead a mixed Gaussian distribution model (Equation 1).

$$G = A_1 \cdot e^{\frac{(x-\mu_1)^2}{2\sigma_1}} + A_2 \cdot e^{\frac{(x-\mu_2)^2}{2\sigma_2}}$$

Equation 1: Mixed Gaussian model

By using Gaussians, we can individually parameterize and describe each season, regardless of single- or double-cycle seasonality. The model is parameterized with best-guesses for each Gaussian variable, which are calculated for each year of the data, and limited by prescribed upper and lower bounds.

Seasonal Variables

The mixed Gaussian model outputs three variables for each individual season: A, the amplitude of the Gaussian curve; μ, mean of the distribution; and σ, the standard deviation or spread (Equation 1). These variables can be conveniently ascribed physical meaning by interpreting them as measures of the magnitude/intensity, timing, and duration of each season, respectively. By reducing seasonality to three simple measurements, isolating change within regional seasonal cycles becomes much more straightforward, as does developing a clear large-scale picture of the seasonal and long-term movement of the ITCZ.

Goodness of Fit

In the interest of quantifying the degree to which our proposed theoretical model provides a useful alternative to simply evaluating seasonality directly from observations according to previous methods, we performed a number of statistical tests that were applied to both randomly generated data and real observations.

For the first test, a year of false monthly precipitation measurements was generated using parameters derived from real observations plus a noise element. The subsequently applied Gaussian model represents that "data" relatively well (Figure 8), providing support for the theory underlying our proposed model. The second test, a chi-squared analysis performed on the entire real dataset, produces less supportive results. In every region, our proposed model fails the chi-squared test. Because the model is applied to every discrete year within the data set, this result could be attributed to the low number of data inputs per model application in conjunction with elements of noisiness not

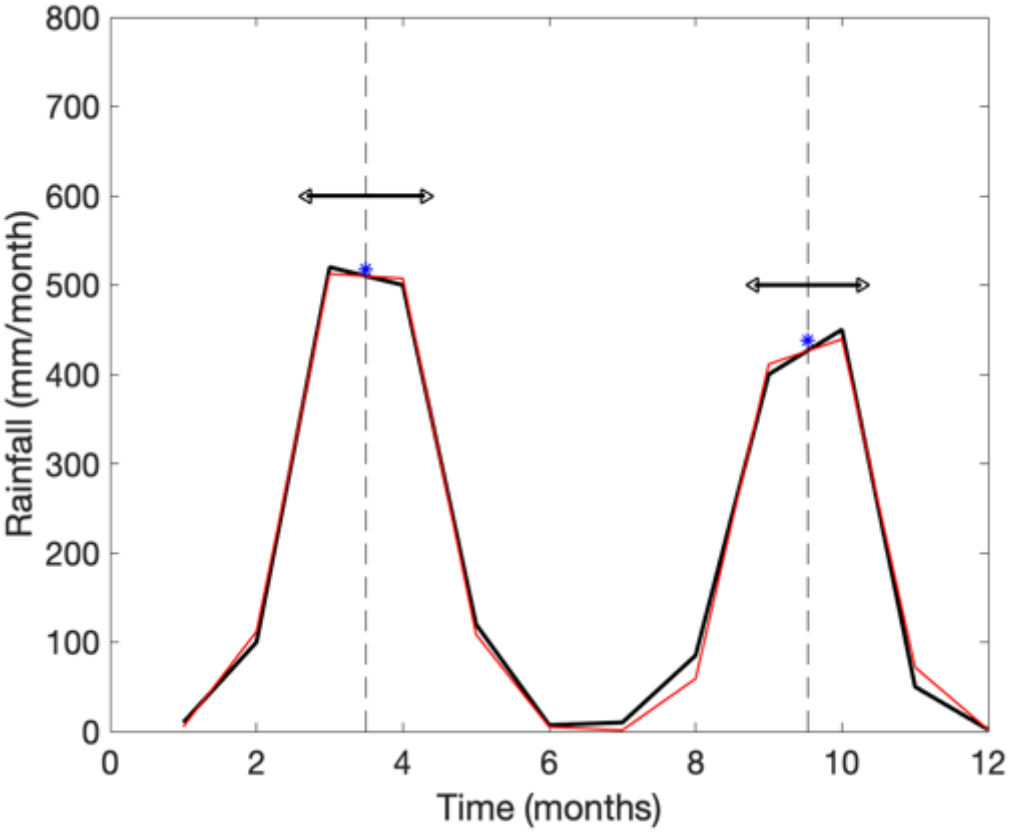

Figure 8: Proposed mixed Gaussian model (red) fit to twelve months of generated data (black). Dashed vertical lines represent the mean value of each distribution, blue stars indicate the amplitude, and black arrows capture the spread, representing the timing, magnitude, and duration of each season, respectively.

appropriately captured by the randomly generated false data from the first test. Though the guiding parameters for the fitting process are derived anew for every site in every year, there is certainly still room for improving the parametrization of the Gaussian model, an issue we hope to address outside of this thesis. For now, the use of our proposed model is narrowly defined and unique enough to continue employing it to describe seasonality—even if the observational data are not truly normally distributed, the model's ability to capture the characteristics of the peaks and troughs in the data remains useful.

Subsequent tests were carried out to test the variance of the model's outputs against a trend analysis of each model output variable. For timing (μ), in particular, the results of this set of tests are telling. Slightly more than half of the modeled GHCN sites (59%) deviated more than a month from the baseline timing parameter suggested during the fitting process at least half the time, suggesting that either the Gaussian framework is not a good method for capturing season timing (unlikely), or that the model requires a different, more well-matched initial parameter (more likely). Only 4% of sites' mode relative to the parameterizing timing value was above one month, only 2% of sites' maximum distance from the suggested value was above one month, and only 1% of sites median distance was above one month, suggesting that for the most part, though many sites express some high variance from the suggest value, few of those sites are dominated by such variance.

Plenty of room for improvement exists regarding the mixed Gaussian approach to quantifying seasonality, particularly in choosing appropriate parameterization values. Nevertheless, the goodness of fit tests described above and the general agreement of the

model's outputs with regional behavior identified by earlier studies substantiate our decision to continue implementing this model.

3. Regionalization

To address spatial data variability and to more purposefully apply our proposed model, we chose to subdivide data sites into representative behavioral groups. Doing so allowed for the individual examination of relatively homogenous regions, which minimizes the pitfalls of comparing sites with disparate time series. Regionalization also presents the opportunity to clearly distinguish between sites which display a double-cycle seasonality and those which display a single-cycle distribution (Figure 9). We tested three different regionalization methods, seeking an option that captured both global and

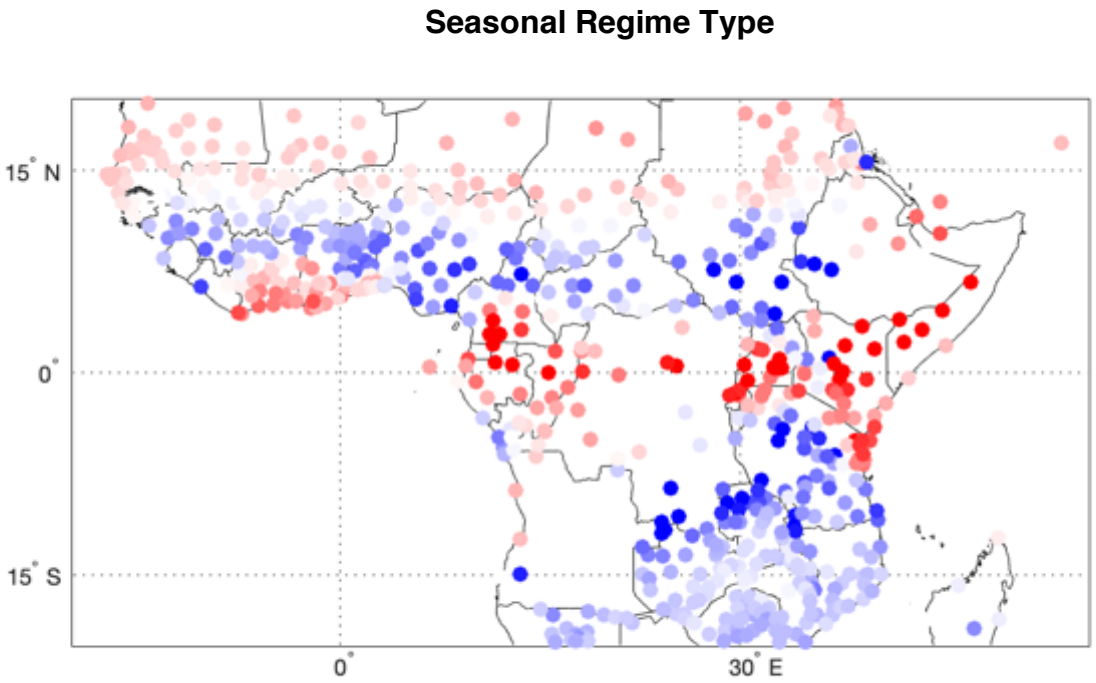

Figure 9: Spatial pattern of sites separated by seasonal pattern using the Fourier harmonics ratio. Sites expressing a double-rainy seasonal cycle are shown in red, while sites expressing a single-rainy season are shown in blue.

regional influences: 1) Fourier harmonic ratios (Yang et al. 2015); 2) k-means clustering based on the mean annual cycle; and 3) the statistical climate regionalization package *HiClimR* (Badr, Zaitchik, and Dezfuli 2015).

Fourier Harmonics Ratio

Before beginning an in-depth regionalization process, it is necessary to understand which broad seasonality pattern each individual site expresses; while the zonal pattern of double seasonal cycles along the equator and single cycles to the north and south can be ascertained using various methods and is widely accepted, a simple generalized understanding of this spatial distribution is useful only to a certain point. In order to classify each site as either doubly or singly seasonal, we have employed a method outlined by Yang et. al (2015). In their study of annual precipitation cycles in the Horn of Africa, they use an index of modality to present a spatial distribution of annual patterns. The index takes the log of a ratio between the annual and semi-annual periodic harmonic functions at each point in a gridded dataset (Equations 2-4).

$$C_1 = \left| \frac{1}{12} \cdot \sum R_m \cdot \ e^{-\left(\frac{2\pi i m}{12}\right)} \right|$$

Equation 2: Annual seasonal harmonic

$$C_2 = \left| \frac{1}{12} \cdot \sum 2 \cdot R_m \cdot \ e^{-\left(\frac{4\pi i m}{12}\right)} \right|$$

Equation 3: Semi-annual seasonal harmonic

$$F_s = \log_2 \left({}^{C_2}/_{C_1} \right)$$

Equation 4: Fourier ratio

If the site most strongly expresses the annual harmonic (Equation 2), the ratio will be less than 1, and the index (F_s in Equation 4) will have a negative value. Conversely, if the semi-annual harmonic (Equation 3) dominates, then the index will have a positive value. The larger the magnitude of the index, the more strongly the site experiences the respective seasonal pattern. For this study, the index calculation has been applied to each individual site, and the results, which clearly confirm the zonal distribution of each pattern, are presented in Figure 9.

K-means on the Annual Cycle

As Badr et. al. (2015) note, climate regionalization is critical in studies seeking to explore the influences and drivers of climatic variables. Defining contiguous geographic and behavioral regions creates an investigative space for relatively simple inquiries related to climate variability and the differences between regions across multiple variables. Combining this logic with knowledge gleaned from the literature, we determined to sort the sites into regions of most similar annual cycle; in other words, though the Fourier harmonics method used broad brushstrokes to differentiate between precipitation behavior within the study region, finer analysis required us to define regions that "rained together," rather than just the same number of times a year. To do so, we initially tested a k-means clustering algorithm on standardized mean annual cycles at each site, with the goal of simultaneously maximizing regional intracorrelation while minimizing intercorrelation between distinct regions. The algorithm requires an arbitrary choice of the number of regions desired; we performed tests requiring between 3 and 20 regions, eventually settling on 10 regions, as that number resulted in the most optimal

distribution of sites between clusters and the most accurate representation of cluster members by the standardized mean annual cycle.

HiClimR

The primary shortcomings of the k-means method described above are the arbitrary choice of number of regions and the method's inability to regionalize based on both the annual cycle and interannual variability. While sorting by mean annual cycle creates regions that experience rain at similar times throughout the year, this parameter alone does not give any indication of change over time. Because we are interested in examining regions that may also be experiencing similar shifts in their seasonal pattern, a parameter of interannual variability must also be included. It is important to note that the k-means method can be applied for interannual variability in the same manner as for the mean annual cycle, but the resulting "regions" are extremely geographically discontinuous. For an accurate and physically logical regionalization, both interannual variability and the mean annual cycle must be taken into account. To achieve this level of comprehensiveness, we look to the recently developed climate regionalization package, *HiClimR* (Badr, Zaitchik, and Dezfuli 2015).

Developed with the explicit intent to provide a flexible tool for climate regionalization, *HiClimR* provides a framework within which to not only regionalize, but also to pre- and post-process data—a feature that becomes exceptionally useful in studies of classically noisy climate parameters, such as precipitation. The package is capable of employing a number of clustering methods; these include Ward's minimum variance and average linkage methods, which have been commonly used in previous climate-related work, as well as new "regional linkage" method designed specifically for climate studies

(Badr, Zaitchik, and Dezfuli 2015). In the context of this study, Ward's method is most applicable to our standardized data and maximizes intraregional correlation while providing the greatest visual agreement of all trials presented by Badr et. al (2015).

Additionally, we required *HiClimR* to both enforce a minimum region size of 50 sites and to apply a contiguity constant of 0.5, thereby eliminating geographic outliers. To further overcome concerns regarding the geographically uneven distribution of GHCN

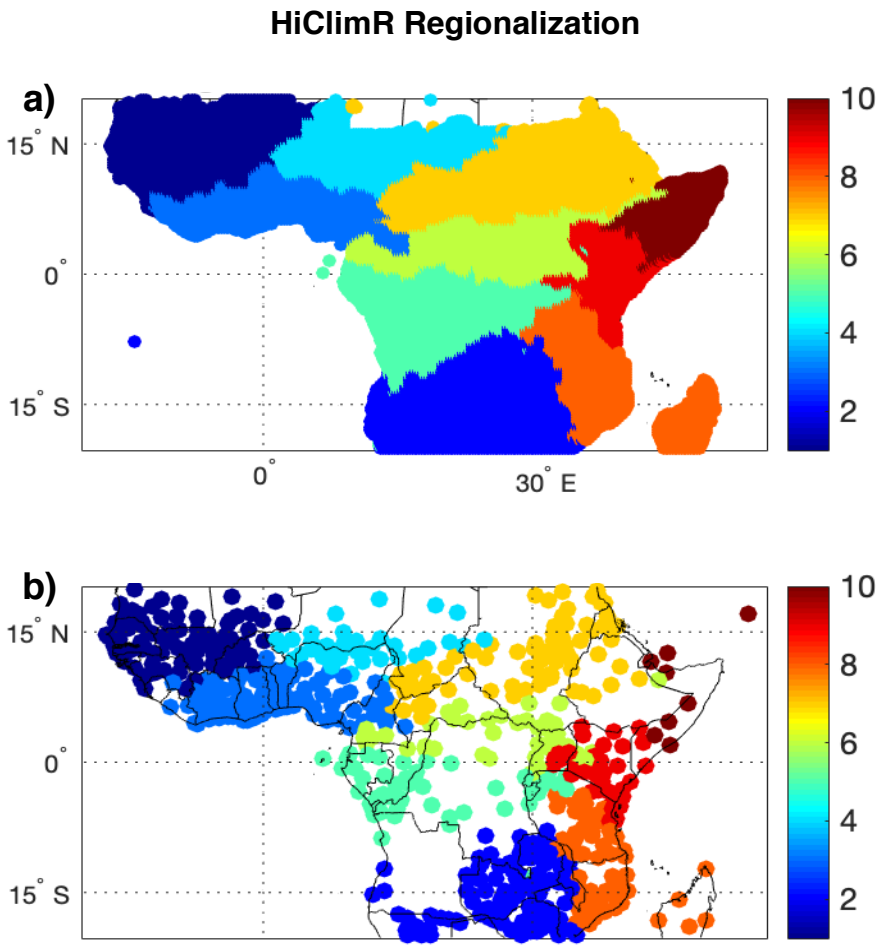

Figure 10: Regionalization of Equatorial Africa by mean annual cycle between 1998 and 2018 according to (a) the statistical package HiClimR using monthly precipitation measurements from the TRMM data set and (b) applied to the GHCN data used in the rest of the seasonal analysis.

data sites, we performed the initial clustering using TRMM data and then snapped the GHCN sites to the output by aligning the coordinates from the *in situ* measurements with the nearest discrete grid point in the satellite data. The resulting regionalization enabled a more minute examination of seasonal variability within the context of our larger investigation (Figure 10).

4. Analysis

Further analysis of seasonality within this study falls into three general areas of concern. First, we performed a trend analysis to identify change over time in each seasonal parameter. Second, we utilized a principle component analysis to explore regional behaviors and situate our findings within the existing literature. Finally, we made use of multiple strategies to isolate the position of the ITCZ and the tropical rain belt, with the intent of better characterizing related seasonal effects.

Trends

After obtaining the output variables for the timing, magnitude/intensity, and duration for each year of observations, we grouped them by region. Continuing from the assumption of homogeneity built into the regionalization process, the outputs were simplified to regional timeseries by averaging values across sites within respective regions. The resulting timeseries were plotted by region and season (boreal spring or fall) and fit with a linear model.

Principle Component Analysis

Significant correlations of the principal components of precipitation timeseries with various regional and global climate influences have been well demonstrated in the

literature (Camberlin 2018; Dezfuli 2017; Nicholson and Dezfuli 2013; Dezfuli and Nicholson 2013; Tierney et al. 2013). To expand this work, we sought to characterize the influences most strongly correlated with each of our derived seasonality metrics. Each regional model-based timeseries was broken down into principal components, of which we consider only the most prominent five. Those components were then each correlated with a set of global climate influences frequently presented in the literature. These include the El Niño index, the Atlantic Meridional Mode, the North Atlantic Oscillation, and the Indian Ocean dipole.

Rain Belt Location

The tropical rain belt, discernable through precipitation measurements, can also serve as a general proxy for the location of the ITCZ. However, it is important to keep in mind that recent work has shown that the two are not as interchangeable as past literature implies (Dezfuli 2017). While this consideration is important to a first order, the ITCZ remains a significant control on equatorial rainfall, as we have argued previously. We therefore continue to infer that changes in average latitude of precipitation correspond well to synchronous changes in the location of the ITCZ.

To calculate a proxy for rain belt positioning, we interpolated the GHCN data network over a 150x150 grid and averaged precipitation values across longitude, producing a representative latitudinal scale for each month of each year. Using the timing of seasonal rainfall as our proxy, we compiled a yearly timeseries for the boreal fall and spring and fit each with a linear model. The results of the entire analysis are presented in the next section.

Results

The results of this study are four-fold. First, applying our proposed model to rain gauge measurements across equatorial Africa reveals notable trends in individual seasonality parameters that are indicative of changes in the large-scale behavioral mechanisms which drive rainfall on the continent. Second, we validated a relatively new method of climate regionalization, successfully forming clusters predicated upon both homogeneity of annual cycle and of interannual variability. Third, a principal component analysis of seasonal timing helps us describe variability in timing regimes and identify potential mechanisms of change within distinct precipitation regions. Finally, we use two alternate approaches to bolster the hypothesis that the regional trends are not the result of regional influences alone but can instead also be attributed to the northward movement of the ITCZ. Taken holistically, these results contribute to a more comprehensive understanding of the future of seasonal rainfall patterns along the African equator.

1. Trends in Seasonality Parameters

Timing

Most regions exhibit significant trends in the timing of both the boreal spring and boreal fall rainy seasons, with up to between a quarter and a half a month change observed during the 1936-1988 period of satisfactory GHCN data coverage (Figure 11). The slope of change varies from region to region: Regions 1 and 2, the northern and southern most groupings in the east, both exhibit a shift toward earlier peak timing of

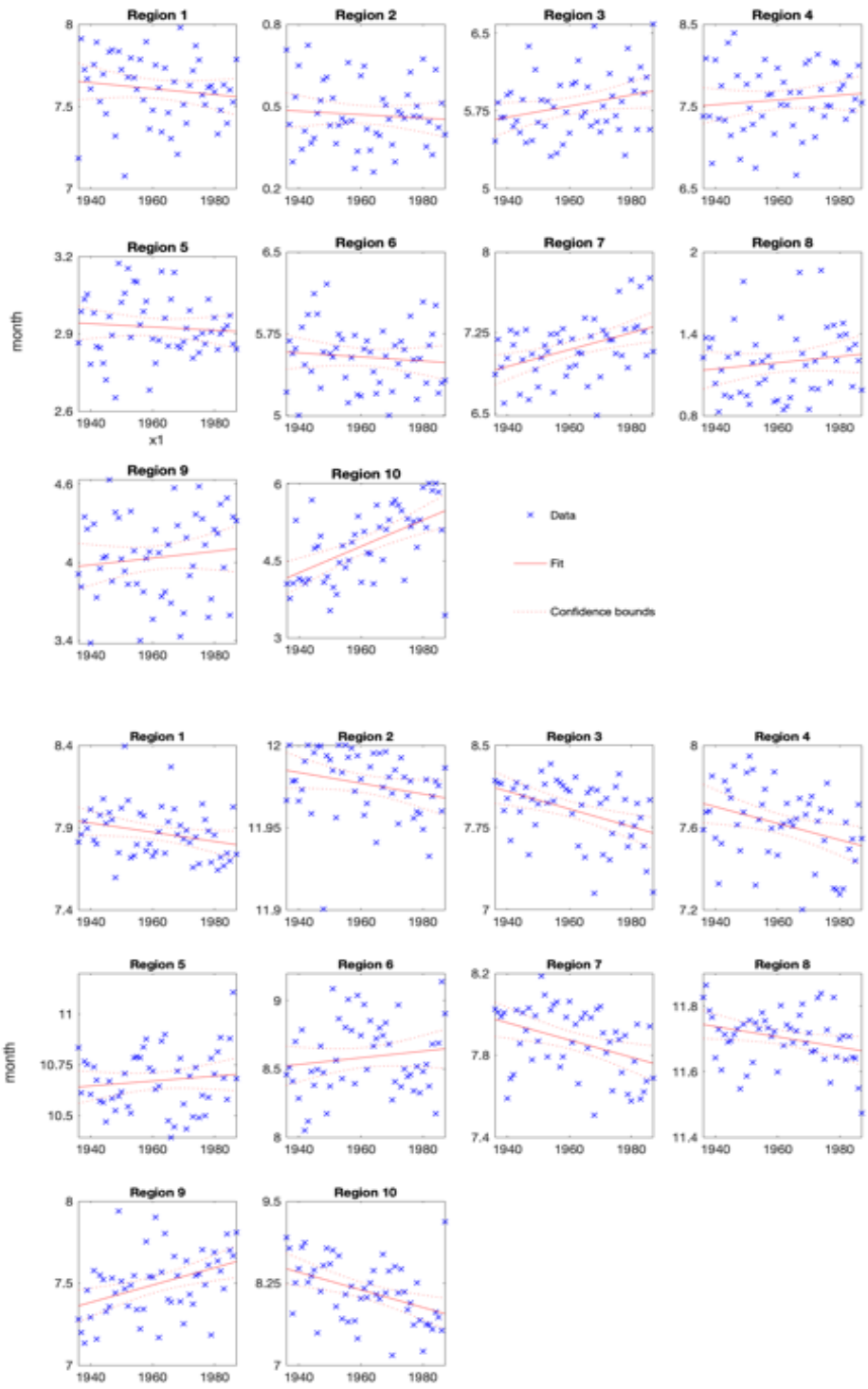

Figure 11: Trends in seasonal timing for each region in the boreal spring (top) and boreal fall (bottom) seasons. Data are shown in blue, the line of best fit is shown in solid red, and the confidence bounds of the fit are shown in dotted red.

both the boreal spring and fall seasons. The boreal spring season in Regions 3, 4, 7, 8, and 10 appears to be peaking later, while the boreal fall season in each of these regions has been earlier. As in Regions 1 and 2, boreal spring in Regions 5 and 6 has shifted earlier, though at a more marginal rate; the corresponding fall seasons, however, have shifted later. Uniquely, Region 9 looks to be experiencing a later seasonal cycle overall, as both the boreal spring and fall peak later on average by 1988 than in 1936.

Qualitatively, the results can be summarized as a later arrival of the boreal spring in most of equatorial Africa, excepting those sites within the Congo River Basin directly along the equator, and the westernmost regions in the northern (where precipitation is heavily influenced by the West African Monsoon) and southern study region. To an even greater degree, most regions are experiencing an earlier boreal fall. Only in Regions 5, 6, and 9, those directly along the equator, has the boreal fall season shifted later in the year. Interannual variability along these trends ranges between approximately 1-2 months, and in nearly all cases, the boreal spring pattern of change inversely mirrors that of the boreal fall pattern, underscoring the cyclically connected nature of annual rainfall in the equatorial region.

Magnitude

Several previous studies have attempted to dispel some of the confusion surrounding the amount of rainfall Africa can expect to see in the coming century (Diem et al. 2014; Schewe and Levermann 2017; Thomas and Nigam 2018; Tierney, Ummenhofer, and deMenocal 2015). Our analysis indicates that the seasonal magnitude— which we use as a generalized proxy for the intensity of seasons and the relative amount of rainfall falling in each—either did not change significantly across the

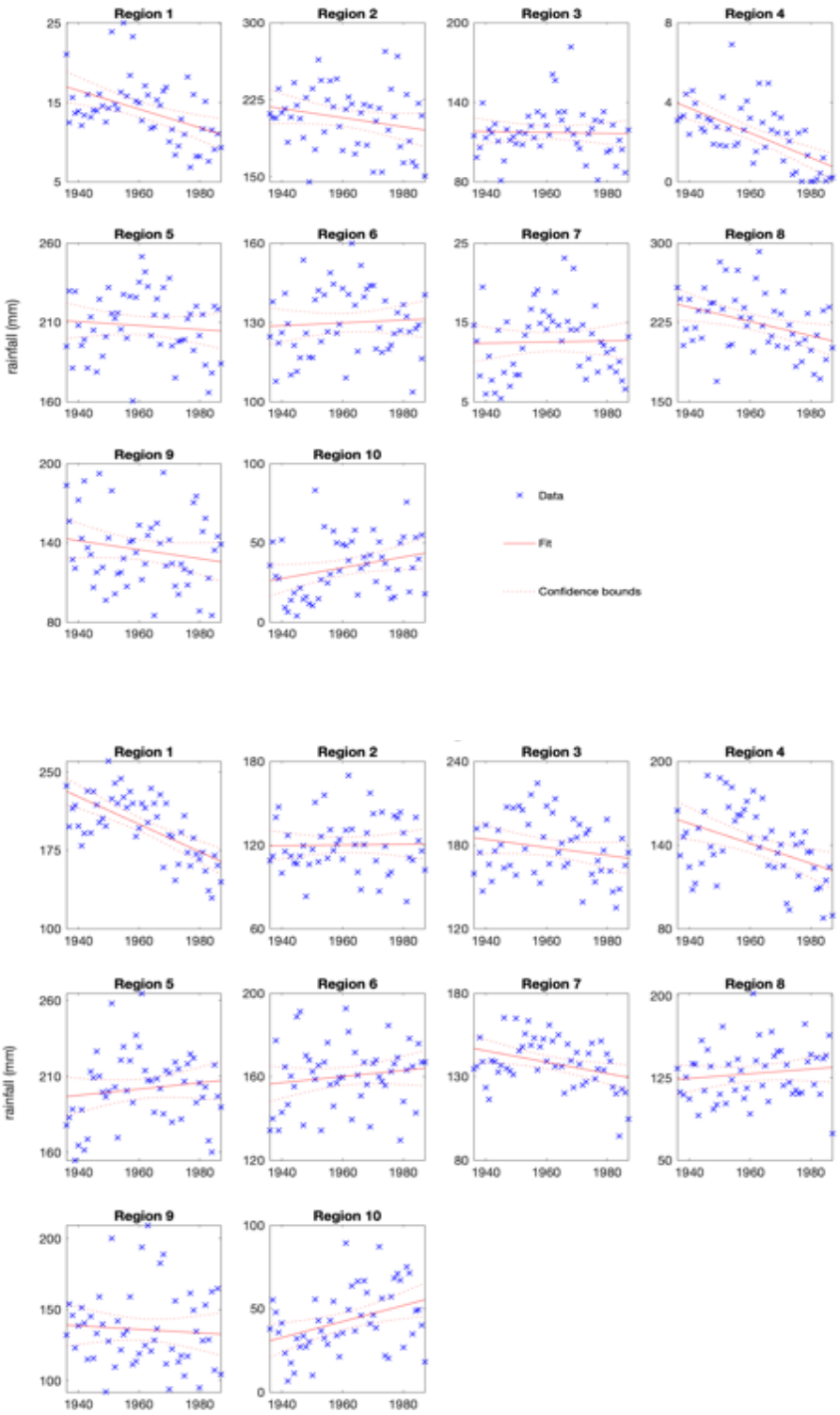

Figure 12: Same as Fig. 11, but for seasonal magnitude.

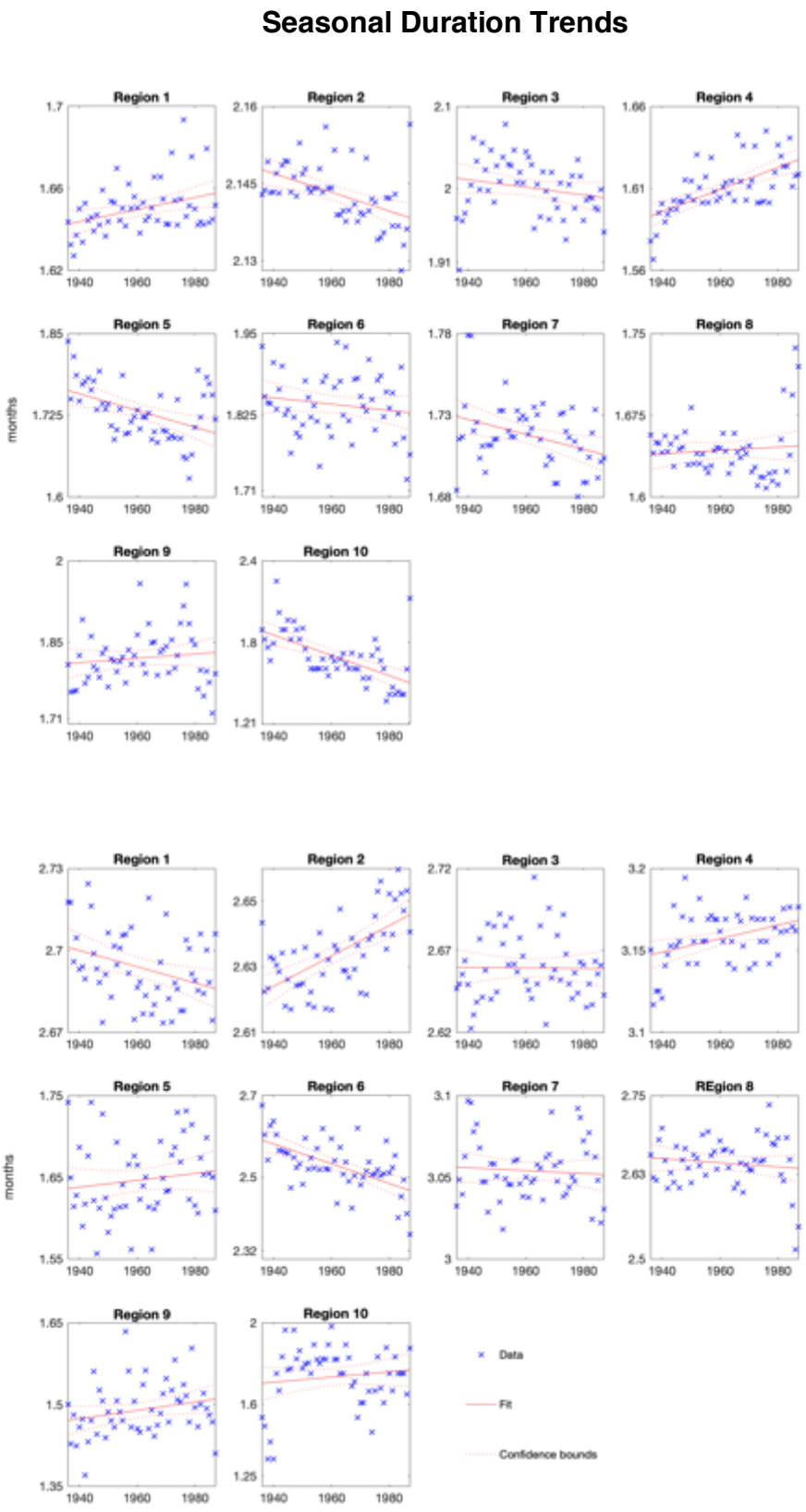

Figure 13: Same as Fig. 11, but for seasonal duration.

equatorial region of Africa or declined between 1936-1998 (Figure 12). The exceptions are both seasons in Region 10 (the GHA) and the boreal fall in Regions 5 and 6 (those sites directly along the equator). This result generally agrees with the conclusions of Thomas and Nigam (2018), who have demonstrated that in the equatorial belt of Africa, wherein rainfall is most abundant, precipitation has been declining and can be expected to continue to do so into the coming century.

Duration

Seasonal duration of both the boreal spring and the boreal fall hovers between one and three months, and changes very little over the course of the study period, often varying on the order of 0.1 months over the entire analysis window (Figure 13). Changes of this magnitude remain insignificant, and duration therefore ranks as the most constant of the three seasonality parameters. What small trends there are appear decoupled from the broad pattern shared by the timing and magnitude trends, exhibiting instead their own particular regional combinations of change across seasons.

The Bigger Picture

Regional results allow us to take a closer look at the bigger picture. Numerous methodologies exist that can be used to study a large-scale system of precipitation like the ITCZ, some of which we have incorporated into our analysis (Armour et al. n.d.; Donohoe et al. 2012; Frierson and Hwang 2012). Taking the puzzle apart piece by piece before putting it back together provides insights into more than just the large-scale mechanism, however. By doing so, the relative contribution of regional, as well as large-scale influences can be inferred, and what might previously have appeared to be unexplainable behavior can reasonably be attributed to sources outside the larger system.

Figures 14 and 15 place the trends discussed above in geographic context, showcasing more clearly the almost totally inverted patterns of change between the boreal spring and fall seasons. This inversion in and of itself implies a single large-scale primary change, as the shifts in one season are mirrored in the other. Qualitatively, we recognize a shift in the northern hemisphere toward a generally later spring season (Figure 14) and the concurrent shift toward a generally earlier fall in the same region.

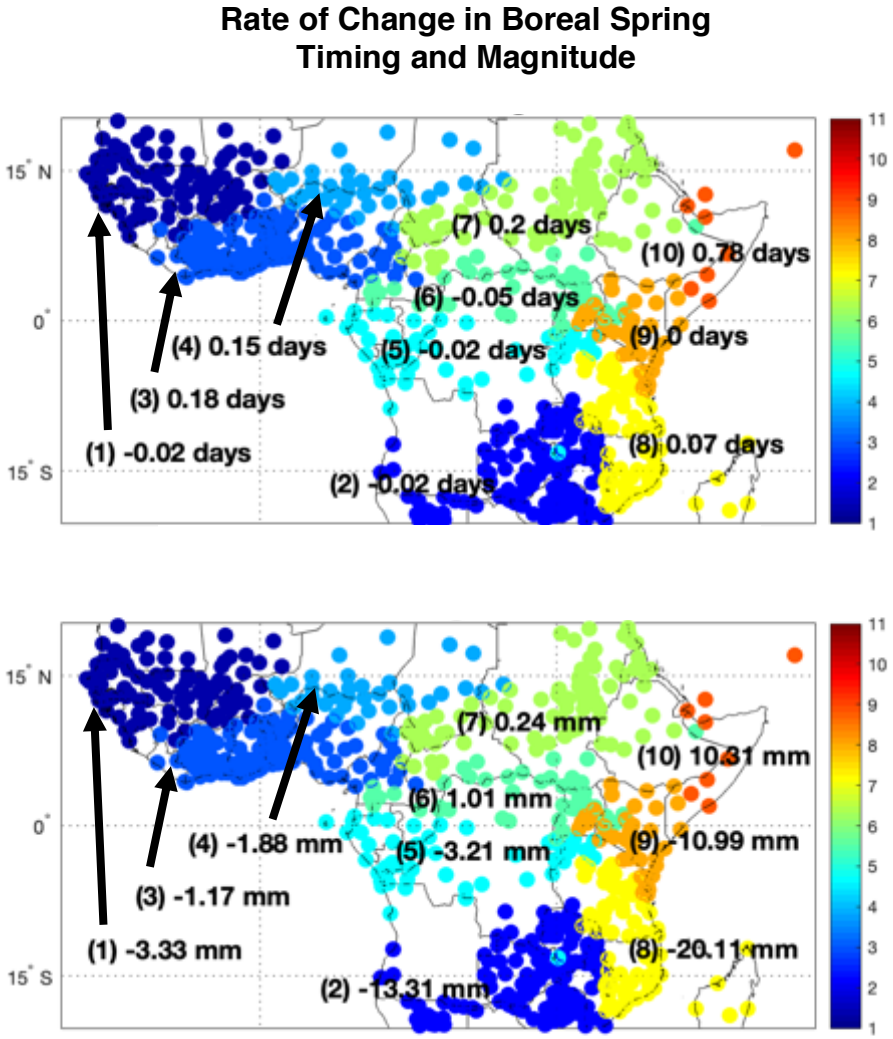

Figure 14: Trends in boreal spring seasonal timing (top) and magnitude (bottom) located by geographic region. Colors represent the numbered regions (1-10). Change in timing is measured in days per year and change in magnitude is measured in mm per year.

(Figure 15). Directly along the equator, a smaller magnitude shift toward an earlier spring timing exists in conjunction with a similar movement toward a later fall season. While considering these trends holistically, one possible explanation is an overall shift northward of the oscillating rain belt's average position, perhaps driven by a higher-order shift in the ITCZ. A change on this sort of scale might help explain shifts in timing of between 0.2 and 0.78 days per year over the half-century examined by this study.

The boreal fall season appears to be drying more quickly than the boreal spring season, though the sub-region directly along the equator is also growing wetter at a faster

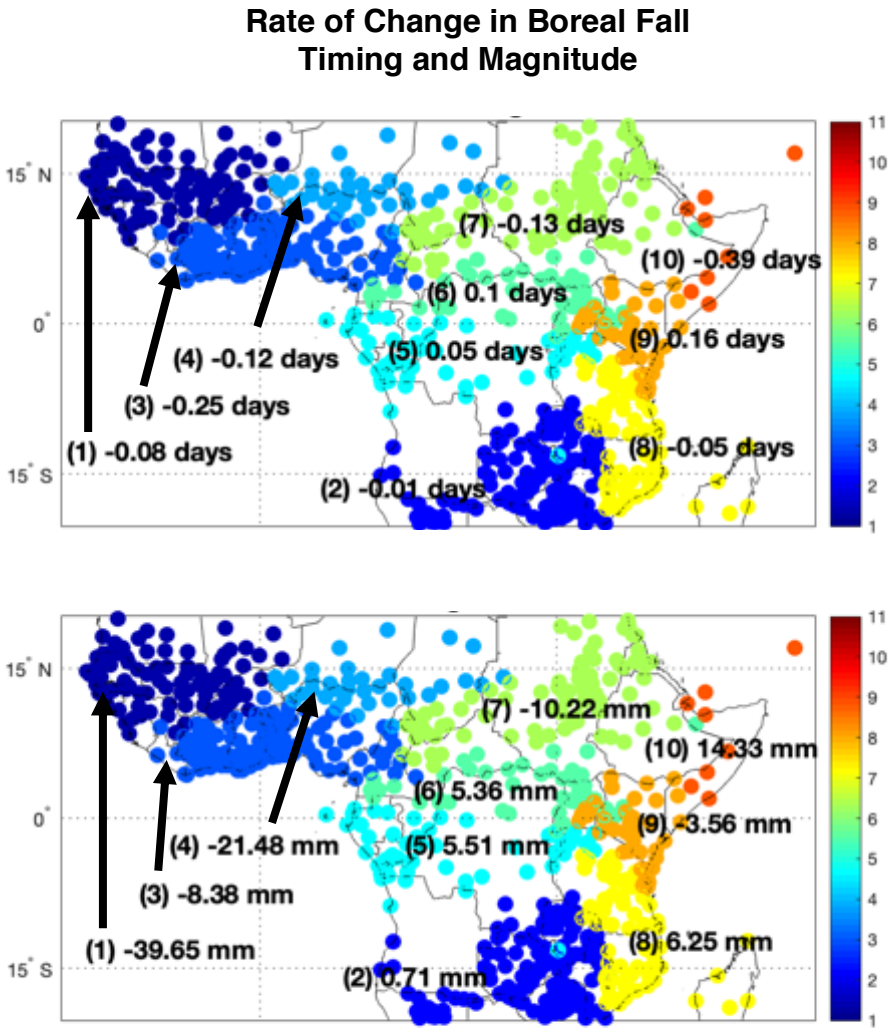

Figure 15: same as Fig. 14, but for the boreal fall.

rate. In the GHA, this supposition is flipped: as both seasons increase in magnitude, the boreal fall season does so more quickly, a result in agreement with regional studies which concluded that the "long rains" boreal fall season in Eastern Africa has been getting wetter.

2. Validation of Regionalization

Applying both k-means clustering and the *HiClimR* regionalization package yields two distinct regional clustering patterns. K-means clustering based on the annual cycle of precipitation (Figure 16) sorts sites into largely longitudinally-contiguous regions, with distinct and numerically few anomalous coastal groupings. While this method effectively reflects the movement of the ITCZ along a latitudinal axis, it neglects the atmospheric and oceanic influences which distinctly modulate the eastern and western regions of the equatorial continent (Dezfuli 2017; Dezfuli and Nicholson 2013; Nicholson and Dezfuli 2013). Though recommended in the related literature, we chose to not calibrate the *HiClimR* package with measures of interannual variability (Badr, Zaitchik, and Dezfuli 2015). The package's authors suggest such use on the premise that it accounts for the influences that alter year-to-year behavior rather

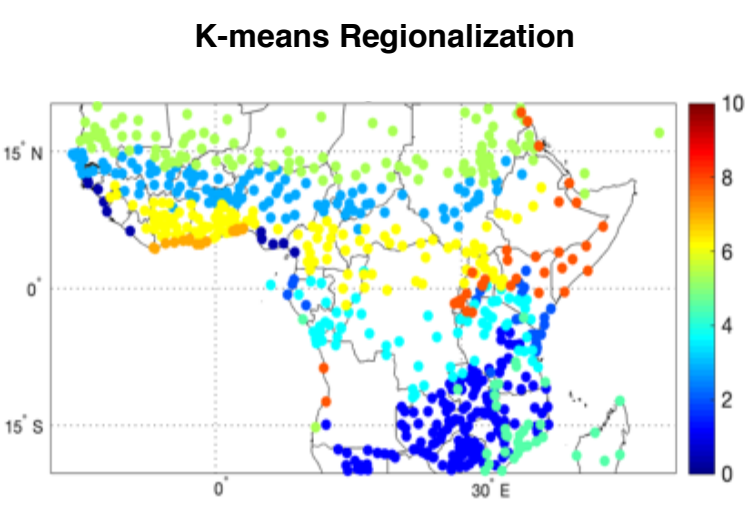

Figure 16: Regionalization of equatorial Africa based upon k-means sorting of normalized annual precipitation cycles. Colors represent individual regions (1-10).

than merely dictating the annual cycle. While capturing these types of influences is desirable, we wished to investigate a group of regions based upon both the similarity of their annual cycle and the simultaneity of their supra-annual shifts. We found that when supplied with the entire, unabridged rainfall record, *HiClimR* segregated sites into regions that reflect both the stratified ITCZ pattern and the globular distribution associated with the distinct east-west effects of regional and global climate influences (Figure 10). The zonal behavior characteristic of the rain belt is still recognizable, but it is overlaid on a longitudinal organization that is particularly prevalent south of the GHA. The two components of our generated pattern agree with distinct and previously separated sets of precipitation influences; together they create a pattern which reasonably approximates a combination of the two.

Unsurprisingly, the rigor of *HiClimR* and its ability to pre-process and appropriately screen data surpass the capabilities of our initial k-means clustering method, creating a more geographically contiguous and climatologically convincing regionalization. Ultimately, we find the *HiClimR* climate regionalization package to be capable of capturing two temporally distinct regional pattern components of seasonality, and we support its employment in future studies.

3. Principal Component Analysis

A principle component analysis is a type of signal processing that decomposes a timeseries into a set of curves which when added together (much in the way sine and cosine curves can be superimposed), recreate the timeseries itself. Each component explains a percentage of the total variance or behavior of the data, and while the principal

component analysis (PCA) can generate as many principal components as there are years in the data set, most of a timeseries' behavior can be accounted for by a few of the first several components.

Timing

The first five principal components of seasonal timing within each region are presented in Figure 17; the associated explanation of variance is presented in Figure 18. During the boreal spring, variance is more equally distributed amongst the first five components, which account for ~35% to 95% of the behavior of boreal spring seasonal timing; with the exception of Regions 2 and 10, the variance curves are quite gradual, with each component contributing between roughly 5% and 15% of the total variance.

Such equal weighting of the primary principal components does not hold true during the boreal fall season. With few exceptions, the first principal component dominates, explaining as much as 50% of the timing variance, and is 10% more explanatory than the next component in over half the regions. More variance overall can be explained during the boreal fall season, 50% to 95%. Despite this pattern in the fall season, it is apparent that a number of factors carry meaningful weight when it comes to setting the peak timing of a rainy season in equatorial Africa.

Previous work outlines many of the regional drivers of precipitation, from sea surface temperatures to zonal wind to atmospheric teleconnections and pressure systems (Camberlin, Janicot, and Poccard, n.d.; Dezfuli and Nicholson 2013; Maidment, Allan, and Black 2015; Nicholson and Dezfuli 2013; Nicholson and Kim 1997; Tierney et al.

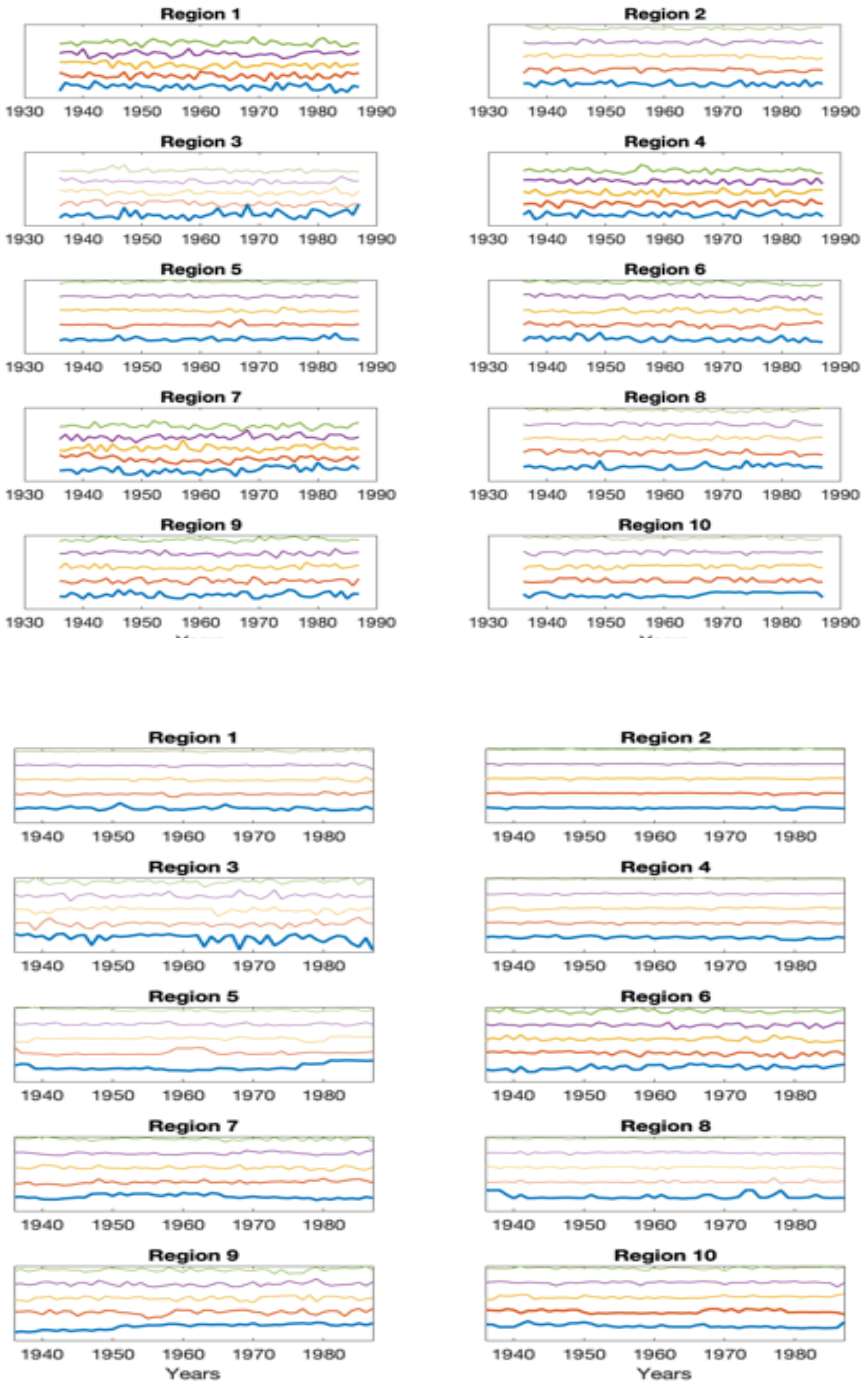

Figure 17: First five principal components of seasonal timing for the boreal spring (top) and fall (bottom). The first component is shown in blue, the second in red, the third in yellow, the fourth in purple and the fifth in green, and the thickness of each line corresponds to the percent of variance explained by each component.

2008; Tierney et al. 2013). Correlations with four such influences, a check on whether known climate drivers were also present in our derived seasonality measurements, are presented in Table 1 (Appendix A). All regions exhibit near-identical timing correlation patterns with the Niño 3.4 index and the North Atlantic Oscillation (NAO) . Generally, these correlations are low, but they are nonetheless convincing conveyers of the contributions of these climate indices. Low values are likely the result of some combination of our seasonal parameters origination from noisy data, the proxy nature of

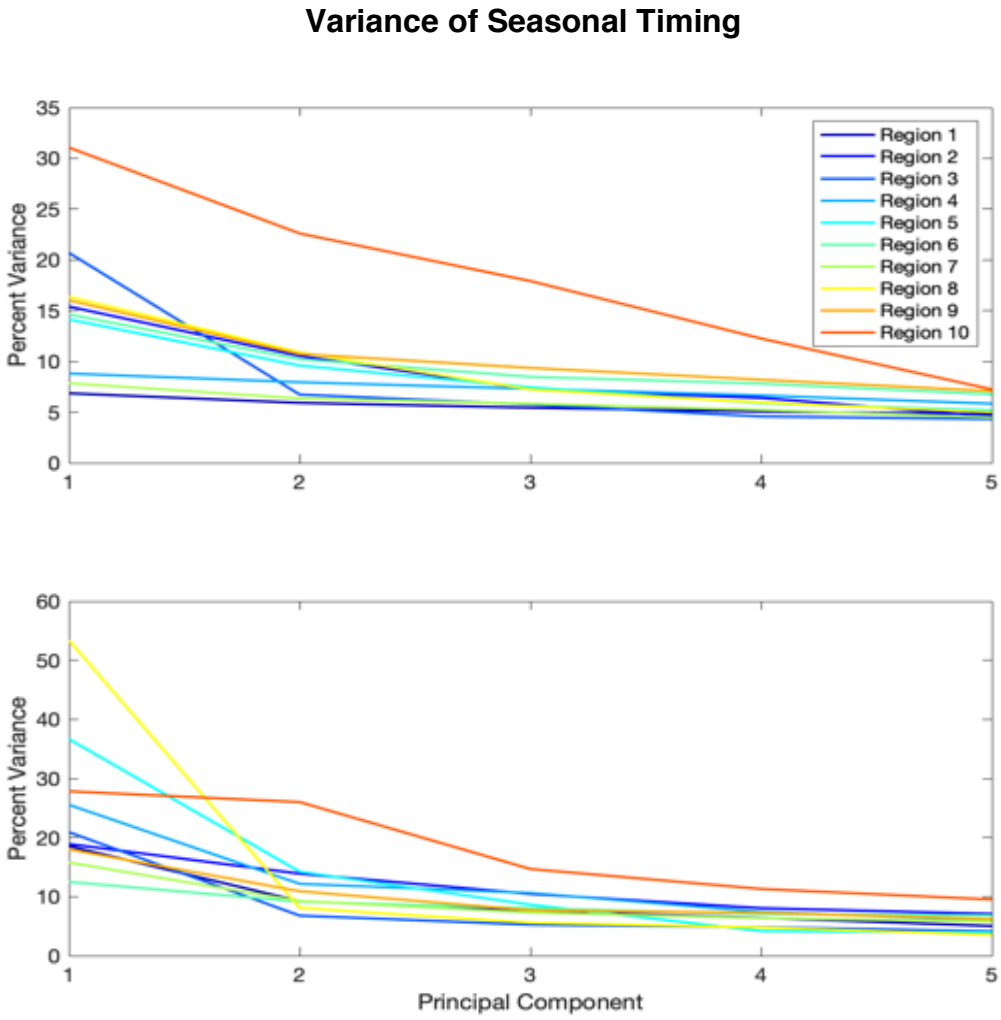

Figure 18: Variance explained by five principal components of seasonal timing for the boreal spring (top) and boreal fall (bottom) seasons. Regional results are indicated by lines of color.

sea surface temperature as a non-direct climate influence, and the overall secondary organizational structure created by these four influences.

Magnitude

A large amount of variance can be explained by the first five principal components in the case of seasonal magnitude, between roughly 50% and 95% in both the boreal spring and fall seasons (Figure 19). The first component of magnitude is also

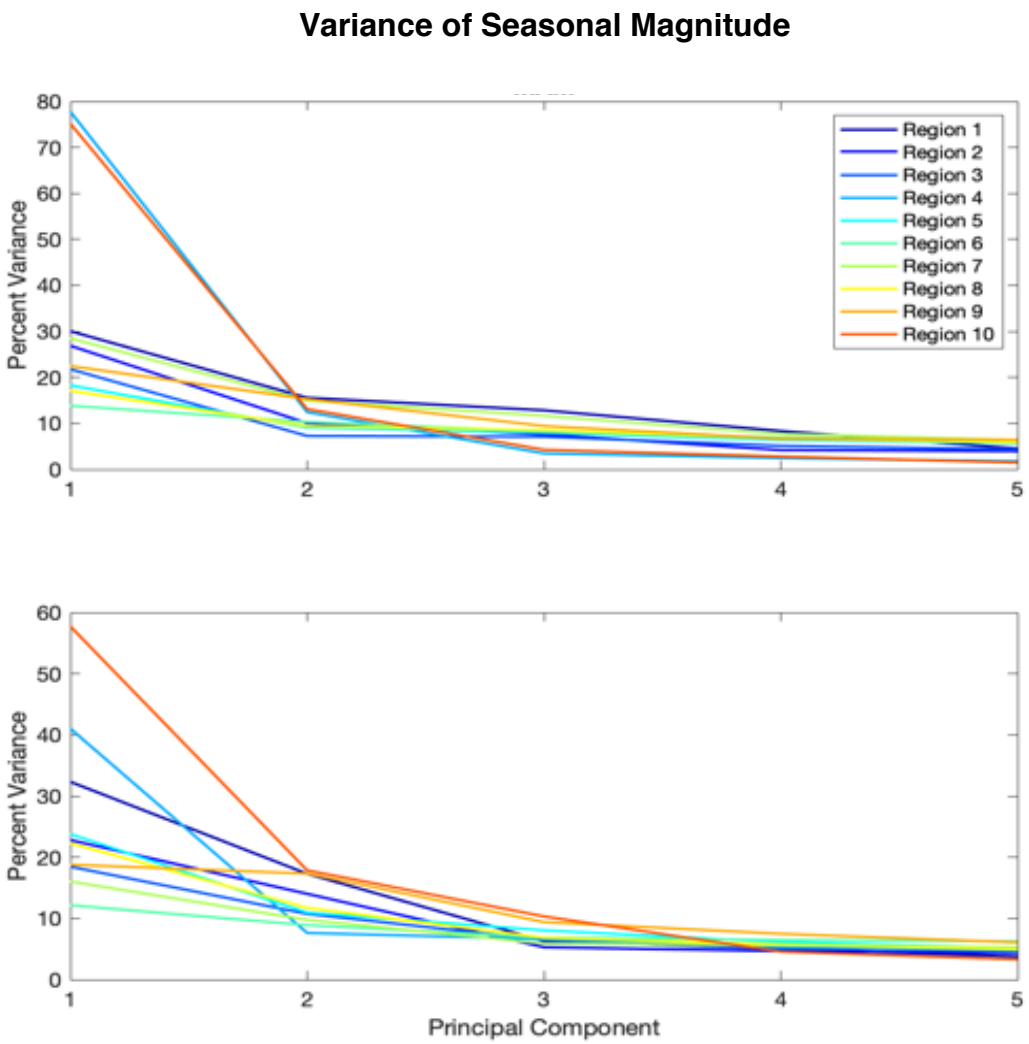

Figure 19: Same as Fig. 18, but for seasonal magnitude.

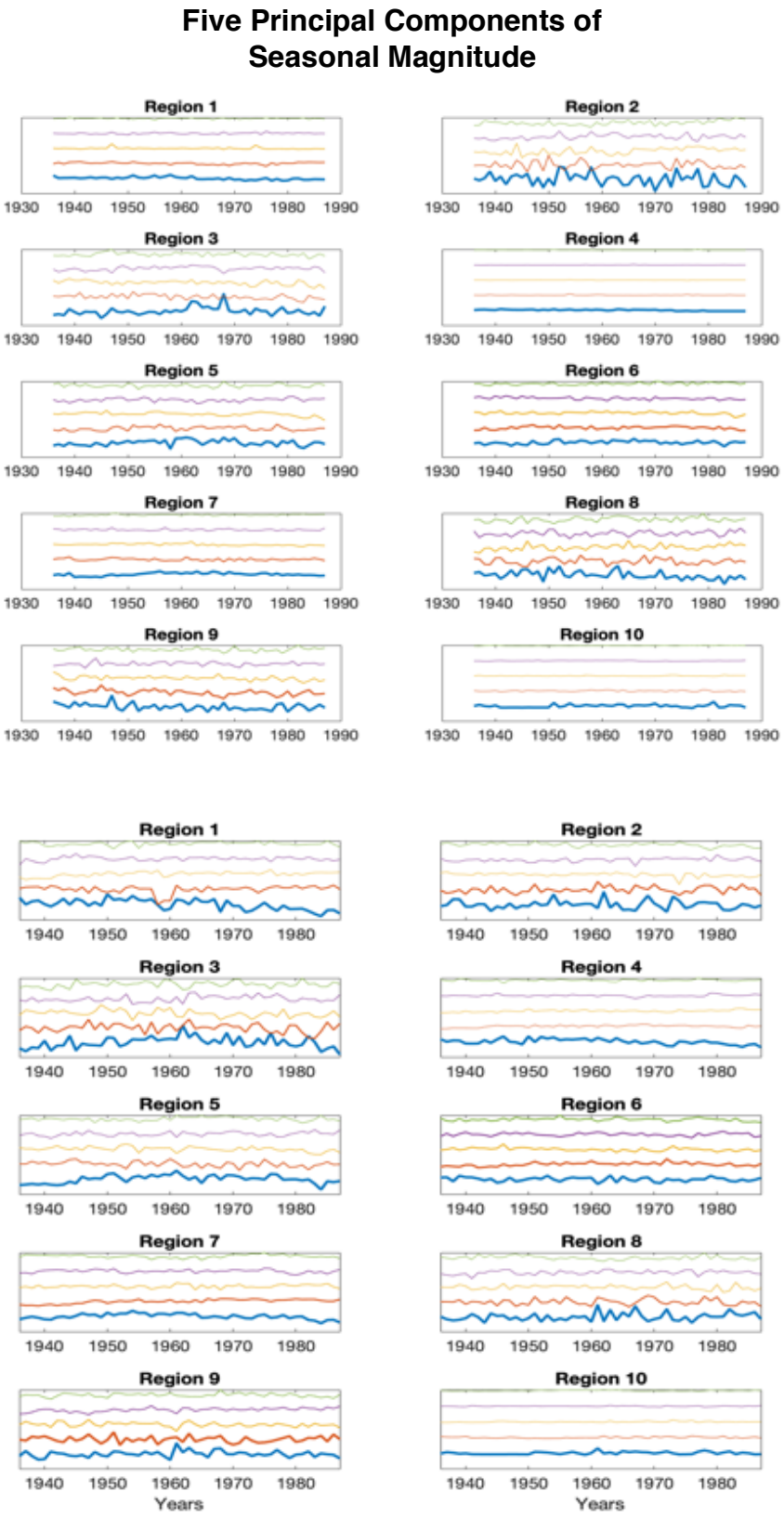

Figure 20: Same as Fig. 17, but for seasonal magnitude.

much more dominantly weighted than that of timing, accounting for more than 70% variance in some cases, implying more single-sourced control on magnitude.

On the other hand, correlations of seasonal magnitude with our chosen four climate indices are generally lower than those of seasonal timing, seldom achieving better than R^2= 0.3 (Table 2, Appendix A). The few exceptions are more significant correlations with the Atlantic Meridional Mode across most sites. This result suggests that seasonal magnitude may be controlled at a more regional level rather than by features captured in the global sea surface temperature indices.

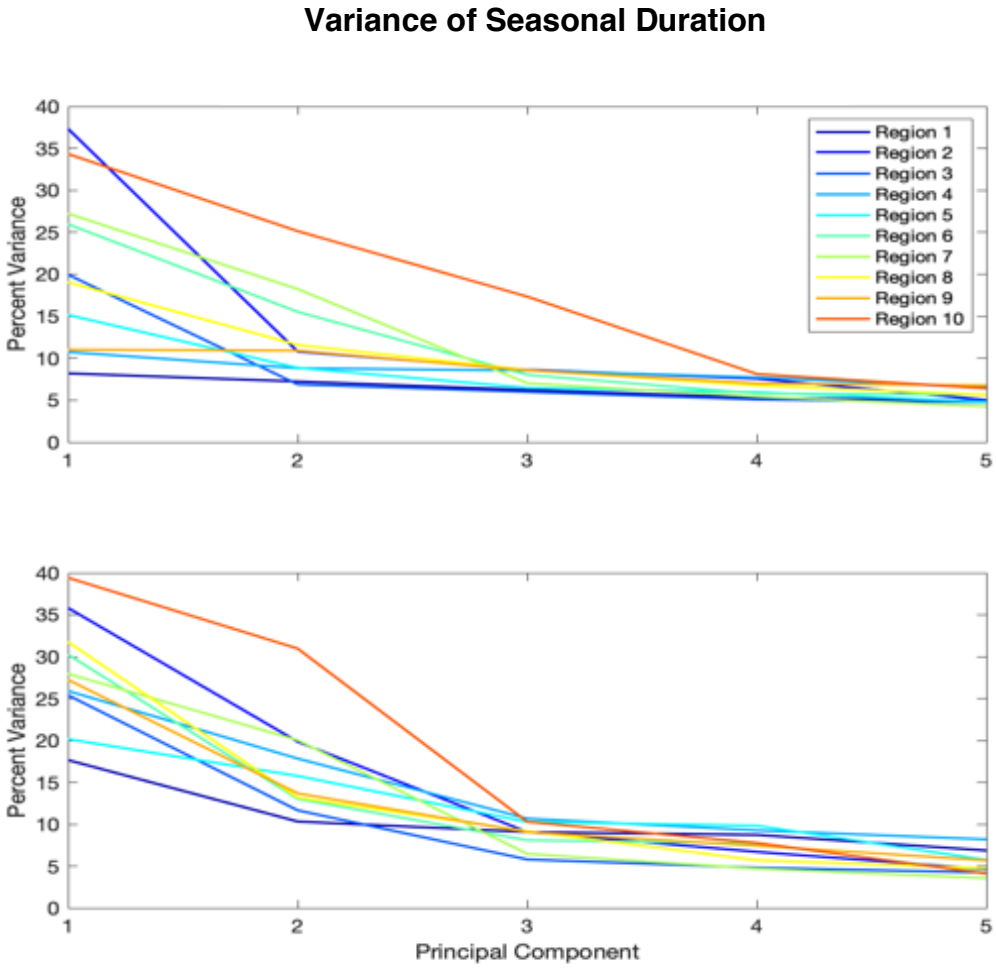

Figure 21: same as Fig. 18, but for seasonal duration.

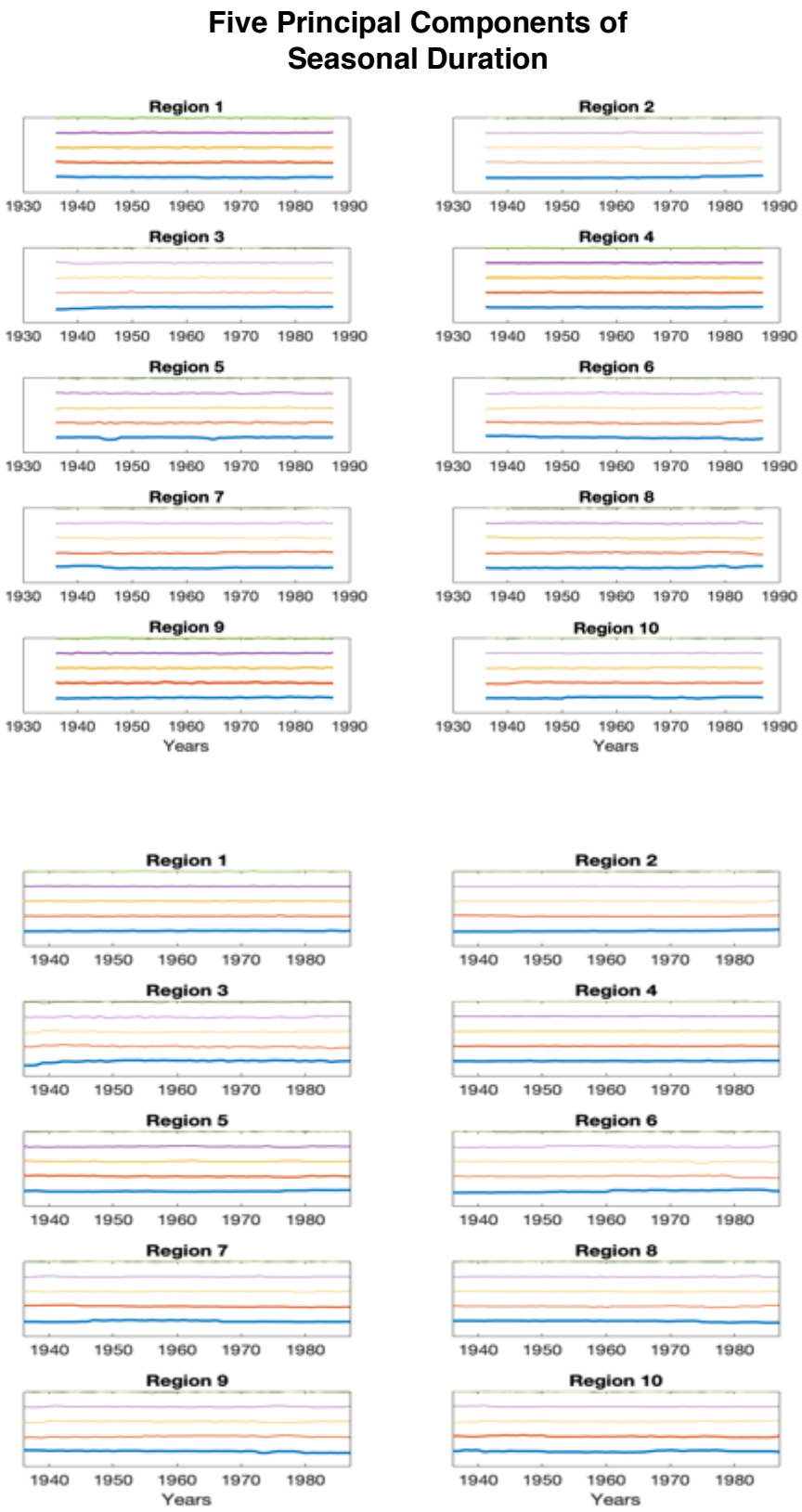

Figure 22: same as Fig. 17, but for seasonal duration.

Duration

The timeseries of the five primary principal components of seasonal duration show extremely little variance, further implying very little change (Figure 22). What variance is captured by the PCA is relatively well-explained by the first five components—between 35% and 90% across all 10 regions (Figure 21)-- and is generally better correlated with the four climate indices than timing or magnitude. Many more of the top two values between the index and the components for each region exceed $r^2 = 0.3$, with multiple instances of correlations surpassing an absolute value of 0.4 (Table 3, Appendix A).

4. Tropical Rain Belt

To scrutinize the implied relationship between the position of the tropical rain belt and the previously outlined regional trends, we isolated a proxy for ITCZ location and compared it to timeseries of the month of equatorial crossing in both rainy seasons. Various proxies to represent the ITCZ exist—we have chosen perhaps the simplest by isolating the month of equatorial crossing of the ITCZ. To do so, we isolated the sites closest to the equator and pulled the zonally averaged peak timing variables for both seasons at those sites in each year of analysis (Figure 24). A further explanation of this process can be found in Appendix B. Both the boreal spring (MAM) and boreal fall (OND) seasons exhibit notable trends. The boreal spring tends toward and earlier crossing over the historical period, while the boreal fall correlates with a later equatorial crossing; in a scenario in which the ITCZ has moved farther north, the time to return to the equator for the fall season would reasonably be longer, and the crossing into the northern hemisphere for boreal spring would be relatively sooner.

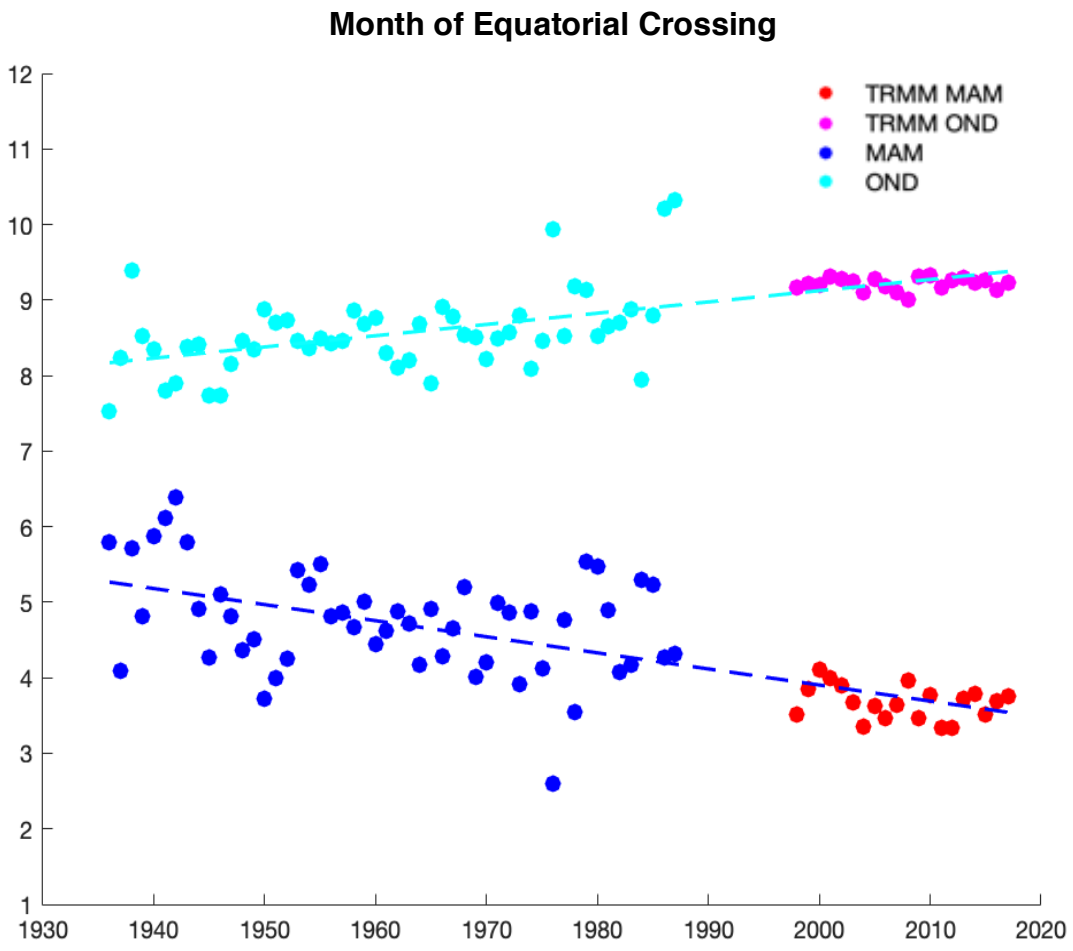

Figure 23: Month of equatorial crossing of the rain belt for the boreal spring (dark blue and red) and boreal fall (cyan and magenta) rainy seasons. The points represent the zonally averaged timing parameter at the equator, and the dashed lines represent the overall trend for each season. TRMM-based timing measurements are appended, to the GHCN record extending the record to the present day. The TRMM record is shown in red for the boreal spring and magenta for the boreal fall.

To check this result and extend our analysis into the satellite period, we performed the same analysis on TRMM-based seasonal timing metrics and appended that record to the historical (Figure 24). The trend convincingly appears to continue into the present day and the changes implied by these trends are visible in maps of seasonal timing during the first and last decades of the study's timeframe (Figure 23), solidifying our conclusion that there has been a real and present overall shift in ITCZ position.

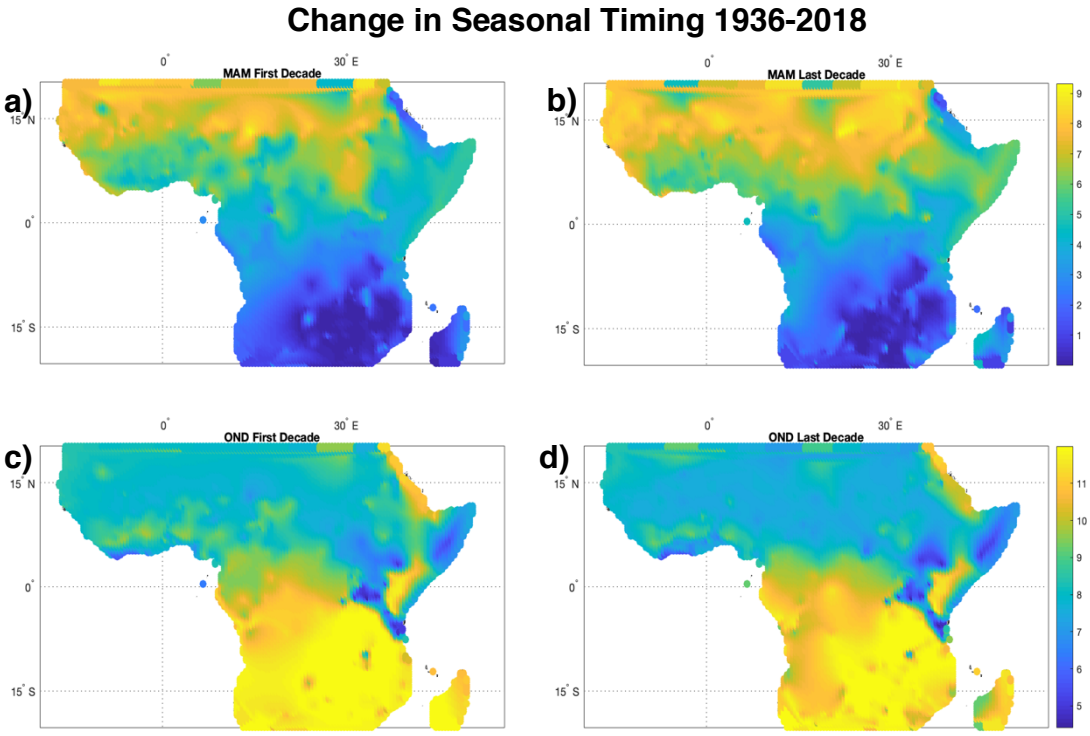

Figure 24: Difference between the 1936-1946 and 2008-2018 averages of seasonal timing for the boreal spring and boreal fall seasons. From top left: (a) 1936-1946 boreal spring; (b) 2008-2018 boreal spring; (c) 1936-1946 boreal spring; and (d) 2008-2018 boreal fall. Yellow colors represent later timing and blue colors represent earlier timing.

Discussion

The results presented in the previous section frame an intriguing and critically important picture of change in equatorial Africa. Our work highlights the need for holistic analysis of the African equatorial region and better solutions to data problems inherent to studies encompassing both historical and modern records. Nevertheless, several different methods used in this study have lent validity to a theorized shift in the average position of the ITCZ over the past century. The consequences of such a change include both real and pressing concerns regarding agricultural adaptability and food resilience for equatorial nations in Africa, as well as a need for continued scientific study of the continental ITCZ in the context of anthropogenic climate change.

1. Model Suitability

As outlined in earlier sections, most common metrics of seasonality already developed in the literature are designed for daily rainfall measurements or based upon a calendric three-month system (Feng et. al. 2015; Liebmann et. al 2007; Seregina et. al. 2019; Yang et. al. 2015). The former condition limits the extent to which historical data, which is primarily available in monthly increments, can be incorporated into a seasonality study, thereby also limiting the temporal scope of analysis. The latter is a blocky, generalized definition that screens important regionally-specific behaviors and changes in seasonality and imposes preconceived notions of timing and duration upon the data. Our proposed mixed Gaussian model of seasonal rainfall could

undoubtedly be improved with regard to achieving optimal statistical rigor, and the method for selecting the most accurate initializing parameters should be debated and fine-tuned. However, the design of the model addresses several recognized shortcomings of previous methodologies.

Seregina et. al. (2018) specifically outline many of these shortcomings, including dependency upon threshold values, inflexibility of definition, and *a priori* determination of the number of rainy seasons in an annual cycle. Their proposed model of precipitation seasonality uses 5-day pentad averages of rainfall to determine the dates of seasonal onset and cessation. These dates are defined relative to a threshold value, which is derived from the climatological annual pattern of each site. For the purposes of the questions we wished to address in the African equatorial region, however, their proposed model is insufficient, due to its inapplicability to monthly precipitation data. The historical record in this thesis' study region also contains many years in which the data record is incomplete, making a valid climatological threshold a difficult statistical requirement. Seregina et. al. also note a tendency toward later (earlier) rainy season onset (cessation) in their model, due to a bias against lighter rain events at the beginning (end) of a season.

Modeling the annual cycle using our proposed model bypasses the need for a threshold by representing seasonal timing as the mean of the distribution, coincident with the peak of rainfall in the season. While the need to pre-determine the number of seasons still exists within our method, the independent parameterization of each distribution allows for a representation of the seasonal cycle that remains accurate and flexible. Finally, this method is well suited to working with discontinuous

precipitation data which may have lower temporal resolution, as it can reasonably model local seasonal behavior and describes seasonality by three simple parameters.

Additionally, our model-based analysis has generated results that are in agreement with both recognized regional patterns of seasonality outlined in the literature and current climate theories (Donohoe et al. 2012; Frierson and Hwang 2012). We therefore conclude that the model still presents an accurate method for representing precipitation in regions known for patterns of single- and double-cycle rainfall patterns.

2. Data Justification

Disparity between *in situ* rain gauge measurements from the historical GHCN network and the more modern TRMM dataset is particularly evident in equatorial Africa. While our proposed model methodology can be flexibly applied to both types of data, the bias of necessarily proxy-based satellite measurements toward precipitation events of a higher magnitude skews the data toward those events which may be considered average events globally, but which fall toward the positive extreme in our study region (Contractor et. al 2015). More conclusively, Contractor et. al. (2015) have also determined that the correlation of satellite precipitation products such as TRMM with *in situ* interpolations are low (between 0.30 and 0.58 in an Australian case study, depending upon the chosen interpolation method). The degree to which these factors may affect the model fit remains slightly unclear but could reasonably drive the mean timing of a season earlier or later compared to gauge data. While this is evident in the narrower spread of TRMM-based seasonal timing,

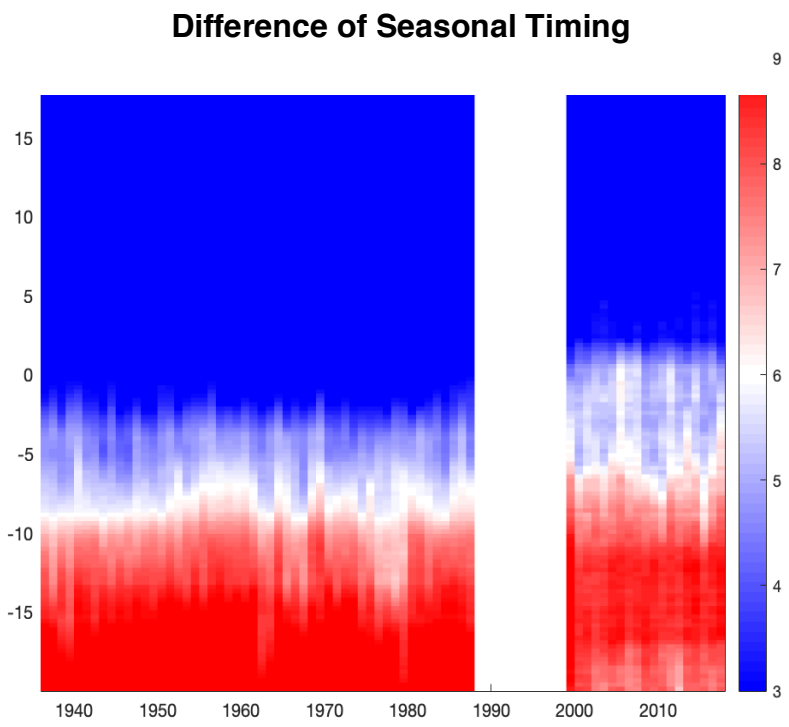

Figure 25: Difference between timing of the boreal spring and boreal fall seasons. Zonal average locations where there is more than 6 months difference between the spring and fall seasonal timing are shown in red; those with less than 6 months difference are shown in blue. The displacement between GHCN observations (1936-1988) and TRMM observations (1998-2018) is obvious, particularly between those sites which have seasonal separations of between 5 and 7 months.

the time associated with equatorial crossing in the satellite period agree with those from the historical record (Figure 24).

While the comparison between TRMM and GHCN holds for the timing of equatorial crossing, displacements between the two become much more dramatic when analyzing the extreme extents of the ITCZ's path (Figure 24). Further work is required to better characterize the discrepancies between historical and satellite records, particularly in regions where low rainfall events are common. Doing so will increase the ability and, hopefully, number of data-based studies, avoiding the pitfalls of using reanalysis products in dry continental regions.

3. Atmospheric Heat Transport and the ITCZ

The patterns of trends in individual seasonal timing across the equatorial region between 1935 and 1988 suggest change related to large scale precipitation mechanisms such as the ITCZ. The literature suggests this is not out of the realm of possibility, but rather a credible reality. Donohoe et. al. demonstrate strong and consistent relationships between atmospheric heat transport and interhemispheric contrast in sea surface temperature with the location of the ITCZ (R^2 = 0.99 and 0.94, respectively) (Donohoe et al. 2012). The idea of global energy balance proffers a simple explanation for these relationships. Energy inputs within the separate latitudinal hemispheres are not equal, but energetic equilibrium demands that the hemispheres become balanced with respect to energy. There are many kinds of energy input, but one of the most prominent, heat, is more prevalent in the northern hemisphere due to the larger land mass and consequent lower heat capacity north of the equator. The global system balances this heat input by increasing atmospheric heat transport across the equator to the south, primarily by way of the ascending branch of the southern Hadley cell. The ITCZ lies where the ascending branches of hemispheric Hadley cells converge and drive air uplift. A northward shift of the ITCZ would bring the southern Hadley cell further into the northern hemisphere and allow greater southward interhemispheric transport. As our data agree to first order with the idea that ITCZ has shifted north, we then further hypothesize that the increasing disparity of temperature between the northern and southern hemispheres due to the asymmetrical effects of anthropogenic climate change may be the driving mechanism behind the aforementioned shift. Current hemispheric temperatures trends support this

Hemispheric Trends in Temperature Change

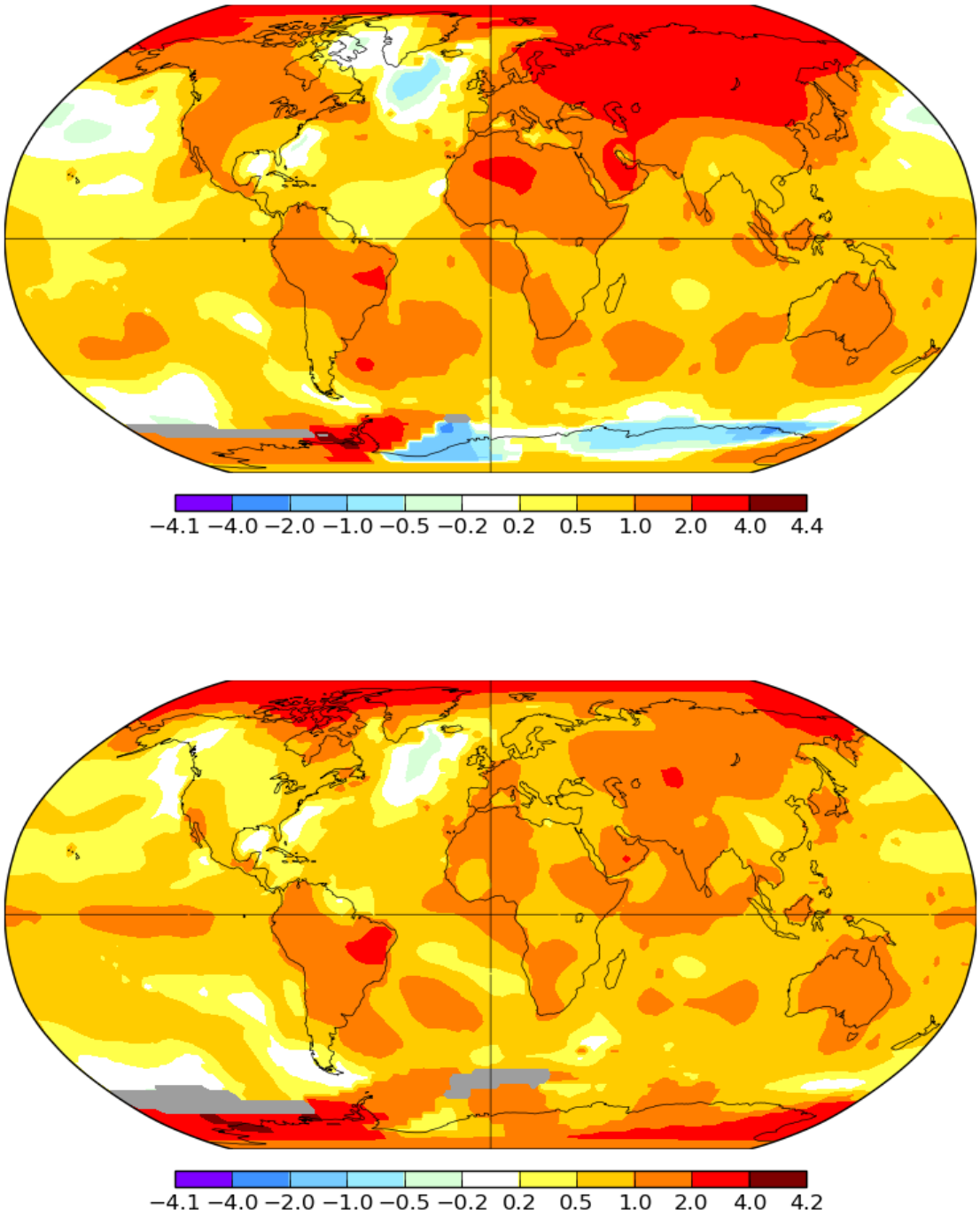

Figure 26: Hemispheric differences in warming from 1936 to 2018 for the boreal spring (top) and boreal fall (bottom). Red colors represent faster warming, while blue colors represent cooling. Image was created using GHCNv3 land temperature and ERSSTv5 ocean temperature data and NASA's GISS Surface Temperature Analysis Global Mapping tool (NASA GISS 2019).

hypothesis, as the Northern Hemisphere warms more quickly than the Southern, particularly in the boreal spring (Figure 25).

Other theories explore the mechanisms necessary to drive a widening of the ITCZ, separate from or in conjunction with a shift, though our data do not explicitly support this idea (Byrne and Schneider 2016). Previous work also confirms that past positional shifts of the ITCZ on similar or larger scales than those proposed by this study have indeed occurred during past cases of global energy imbalance, such as the Last Glacial Maximum and subsequent deglaciation (Arbuszewski et al. 2013)

4. Confluence of Regional and Large-Scale Change

The region-by-region trends in seasonal timing derived from model applications to the GHCN time series at each site can reasonably be interpreted as reflections of the changing positioning of the ITCZ. A noticeable variation from this large-scale narrative includes Region 9, below the GHA, which is broadly consistent with the recognized regional influence of the Indian Ocean and Asian monsoonal dynamics outlined in the literature. Isolating the month of equatorial crossing also implies a difference in the influence of regional drivers between seasons: the narrow spread of points in the boreal fall crossing suggests a more regular or individualized influence relative to the boreal spring crossing, which exhibits much more variance (Figure 24). One interpretation of this result may be that regional influences play a stronger role in determining boreal spring seasonality, while the boreal fall is dictated by a less variable mechanism such as the ITCZ. As such, understanding the nuances of regional influences remains critically important for adaptability within all parts of

the larger region, but so too is contextualizing those influences within larger systems like the ITCZ that are also changing.

We have shown that the average position of the ITCZ may have shifted enough to alter the seasonal timing at the equator by as much as month over the last century. If this pattern generally extends to the rest of equatorial Africa, the ramifications for populations within that area could be substantial. For example, sorghum, the primary subsistence crop in equatorial Africa, has a long maturation period of 90-120 days and is dependent upon high temperatures to maximize photosynthesis. In order to maintain optimal conditions over the entire growth window, avoiding late planting is crucial. While agriculture and crop management depend upon factors other than rainfall alone, an unrecognized change in the ITCZ on the order of months could lead to early or late planting, resulting in poor crop yields.

The wider literature surveyed for this thesis is missing a focus on the continental ITCZ over Africa; continuing to fill this scientific gap will enhance the knowledge base for future adaptability measures, hopefully helping to drive well-informed and applicable policy implementation.

Conclusion and Future Work

We have sought to investigate the real-world possibility that the Intertropical Convergence Zone may be shifting, as is suggested by climate theory and in current global climate models (Bischoff and Schneider 2014; Donohoe et al. 2012; Putnam and Broecker 2017; Schneider, Bischoff, and Haug 2014). Having chosen to limit our analysis to rain gauge data and satellite measurements alone, we have developed a new statistical model which helps to overcome the shortcomings and data gaps in the historical record. More importantly, the model better isolates measurements of seasonal timing relative to previous methodologies; we have used these derived measurements to track change in the large scale ITCZ and the tropical rain belt system over the last century.

Our findings support the theory of a shifting ITCZ. Trends in seasonal timing indicate an earlier boreal spring season and a later boreal fall season across most of the study region, which is likely the result of a northward migration of the ITCZ's average position. Our work therefore suggests that the underpinning theories of global climate models are capturing real-world effects of anthropogenic climate change. Additionally, the livelihoods of most of the population in equatorial Africa will likely continue to be affected by this trend, and continued work should help inform predictions of future change, as well as any adaptability measures that become necessary.

While we present our findings with confidence, there is still much more work to be done regarding rainfall seasonality and the ITCZ in equatorial Africa. A better understanding of how to overcome data discrepancy issues between rain gauge and

satellite measurements is absolutely necessary in order to conclusively examine the historical and modern records using solely observational data. We plan to continue fine-tuning our proposed mixed Gaussian model, focusing on better parameterization techniques and issues related to the low temporal resolution of historical gauge data.

Lastly, we advocate for further investigation of the extreme extents of the ITCZ over the last century, as well continued focus on the physical interactions between the ITCZ and regional and local drivers of rainfall. Such work will reduce the uncertainty of future predictions of change and help inform strategies to strengthen food security across the equatorial African continent.

References

Arbuszewski, Jennifer A., Peter B. deMenocal, Caroline Cleroux, Louisa Bradtmiller, and Alan Mix. "Meridional Shifts of the Atlantic Intertropical Convergence Zone since the Last Glacial Maximum." *Nature Geoscience* 6, no. 11 (2013): 959–62. http://dx.doi.org.ezp-prod1.hul.harvard.edu/10.1038/ngeo1961.

Armour, Kyle C, Nicholas Siler, Aaron Donohoe, and Gerard H Roe. "Meridional Atmospheric Heat Transport Constrained by Energetics and Mediated by Large-Scale Diffusion." Accessed March 7, 2019. https://doi.org/10.31223/osf.io/c4tqx.

Badr, Hamada S., Benjamin F. Zaitchik, and Amin K. Dezfuli. "A Tool for Hierarchical Climate Regionalization." *Earth Science Informatics; Dordrecht* 8, no. 4 (December 2015): 949–58. http://dx.doi.org.ezp-prod1.hul.harvard.edu/10.1007/s12145-015-0221-7.

Balas, N., S. E. Nicholson, and D. Klotter. "The Relationship of Rainfall Variability in West Central Africa to Sea-Surface Temperature Fluctuations." *International Journal of Climatology* 27, no. 10 (2007): 1335–49. https://doi.org/10.1002/joc.1456.

Bischoff, Tobias, and Tapio Schneider. "Energetic Constraints on the Position of the Intertropical Convergence Zone." *Journal of Climate* 27, no. 13 (2014): 4937–51. http://dx.doi.org.ezp-prod1.hul.harvard.edu/10.1175/JCLI-D-13-00650.1.

Byrne, Michael P., and Tapio Schneider. "Energetic Constraints on the Width of the Intertropical Convergence Zone." *Journal of Climate; Boston* 29, no. 13 (July 1, 2016): 4709–21. http://dx.doi.org.ezp-prod1.hul.harvard.edu/10.1175/JCLI-D-15-0767.1.

Camberlin, P., S. Janicot, and I. Poccard. "Seasonality and Atmospheric Dynamics of the Teleconnection between African Rainfall and Tropical Sea-Surface Temperature: Atlantic vs. ENSO." *International Journal of Climatology* 21, no. 8 (n.d.): 973–1005. https://doi.org/10.1002/joc.673.

Camberlin, Pierre. "Climate of Eastern Africa." *Oxford Research Encyclopedia of Climate Science*, January 24, 2018. https://doi.org/10.1093/acrefore/9780190228620.013.512.

Carter, P. R., et al. "Grain Sorghum (Milo)." *Alternative Field Crops Manual*, University of Wisconsin-Extension and University of Minnesota, hort.purdue.edu/newcrop/afcm/sorghum.html.

Chakraborty, Sudip, Rong Fu, Steven T. Massie, and Graeme Stephens. "Relative Influence of Meteorological Conditions and Aerosols on the Lifetime of Mesoscale Convective Systems." *Proceedings of the National Academy of Sciences* 113, no. 27 (July 5, 2016): 7426–31. https://doi.org/10.1073/pnas.1601935113.

Contractor, Steefan, Lisa V. Alexander, Markus G. Donat, and Nicholas Herold. "How Well Do Gridded Datasets of Observed Daily Precipitation Compare over Australia?" *Advances in Meteorology* 2015 (2015): 1–15. https://doi.org/10.1155/2015/325718.

Dezfuli, Amin. *Climate of Western and Central Equatorial Africa*. Oxford University Press, 2017. http://oxfordre.com/climatescience/view/10.1093/acrefore/9780190228620.001.0001/acrefore-9780190228620-e-511.

Dezfuli, Amin K., and Sharon E. Nicholson. "The Relationship of Rainfall Variability in Western Equatorial Africa to the Tropical Oceans and Atmospheric Circulation. Part II: The Boreal Autumn." *Journal of Climate* 26, no. 1 (2013): 66–84. http://dx.doi.org.ezp-prod1.hul.harvard.edu/10.1175/JCLI-D-11-00686.1.

Diem, Jeremy E., Sadie J. Ryan, Joel Hartter, and Michael W. Palace. "Satellite-Based Rainfall Data Reveal a Recent Drying Trend in Central Equatorial Africa." *Climatic Change* 126, no. 1–2 (2014): 263–72. http://dx.doi.org.ezp-prod1.hul.harvard.edu/10.1007/s10584-014-1217-x.

Donohoe, Aaron, John Marshall, David Ferreira, and David Mcgee. "The Relationship between ITCZ Location and Cross-Equatorial Atmospheric Heat Transport: From the Seasonal Cycle to the Last Glacial Maximum." *Journal of Climate* 26, no. 11 (November 12, 2012): 3597–3618. https://doi.org/10.1175/JCLI-D-12-00467.1.

Easterling, David R., and Thomas C. Peterson. "A New Method for Detecting Undocumented Discontinuities in Climatological Time Series." *International Journal of Climatology* 15, no. 4 (n.d.): 369–77. https://doi.org/10.1002/joc.3370150403.

Fagbenle, R.'Layi. "Fourier Analysis of Climatological Data Series in a Tropical Environment." *International Journal of Energy Research* 19, no. 2 (March 1995): 117–23. https://doi.org/10.1002/er.4440190204.

Feng, Xue, Amilcare Porporato, and Ignacio Rodriguez-Iturbe. "Changes in Rainfall Seasonality in the Tropics." *Nature Climate Change* 3, no. 9 (September 2013): 811–15. https://doi.org/10.1038/nclimate1907.

Frierson, Dargan M. W., and Yen-Ting Hwang. "Extratropical Influence on ITCZ Shifts in Slab Ocean Simulations of Global Warming." *Journal of Climate* 25, no. 2 (January 2012): 720–33. https://doi.org/10.1175/JCLI-D-11-00116.1.

GISTEMP Team, 2019: *GISS Surface Temperature Analysis (GISTEMP)*. NASA Goddard Institute for Space Studies. Dataset accessed 2019-04-04 at data.giss.nasa.gov/gistemp/.

Griscom, Bronson W., and Rane Cortez. "The Case for Improved Forest Management (IFM) as a Priority REDD+ Strategy in the Tropics." *Tropical Conservation Science* 6, no. 3 (August 2013): 409–25. https://doi.org/10.1177/194008291300600307.

Haddad, Khaled, Fiona Johnson, Ataur Rahman, Janice Green, and George Kuczera. "Comparing Three Methods to Form Regions for Design Rainfall Statistics: Two Case Studies in Australia." *Journal of Hydrology* 527 (August 2015): 62–76. https://doi.org/10.1016/j.jhydrol.2015.04.043.

Hall, N. M.J., and P. Peyrillé. "Dynamics of the West African Monsoon." *Journal de Physique IV (Proceedings)* 139, no. 1 (December 2006): 81–99. https://doi.org/10.1051/jp4:2006139007.

Hansen, J., R. Ruedy, M. Sato, and K. Lo, 2010: Global surface temperature change, *Rev. Geophys.*, **48**, RG400. https://doi-org.ezp-prod1.hul.harvard.edu/10.1073/pnas.0606291103.

Hulme, M, R Doherty, T Ngara, M New, and D Lister. "African Climate Change: 1900-2100." *Climate Research* 17 (2001): 145–68. https://doi.org/10.3354/cr017145.

Hulme, Mike. "Rainfall Changes in Africa: 1931–1960 to 1961–1990." *International Journal of Climatology* 12, no. 7 (n.d.): 685–99. https://doi.org/10.1002/joc.3370120703.

IPCC, 2013: Summary for Policymakers. In: *Climate Change 2013: The Physical Science Basis. Contribution of Working Group I to the Fifth Assessment Report of the Intergovernmental Panel on Climate Change* [Stocker, T.F., D. Qin, G.-K. Plattner, M. Tignor, S.K. Allen, J. Boschung, A. Nauels, Y. Xia, V. Bex and P.M. Midgley (eds.)]. Cambridge University Press, Cambridge, United Kingdom and New York, NY, USA.

Janowiak, John E., Arnold Gruber, C. R. Kondragunta, Robert E. Livezey, and George J. Huffman. "A Comparison of the NCEP–NCAR Reanalysis Precipitation and the GPCP Rain Gauge–Satellite Combined Dataset with Observational Error Considerations." *Journal of Climate* 11, no. 11 (November 1998): 2960–79. https://doi.org/10.1175/1520-0442(1998)011<2960:ACOTNN>2.0.CO;2.

Kazadi, Sanga-Ngoie, and Fukuyama Kaoru. "Interannual and Long-Term Climate Variability over the Zaire River Basin during the Last 30 Years." *Journal of Geophysical Research: Atmospheres* 101, no. D16 (1996): 21351–60. https://doi.org/10.1029/96JD01869.

Kotir, Julius H. "Climate Change and Variability in Sub-Saharan Africa: A Review of Current and Future Trends and Impacts on Agriculture and Food Security." *Environment, Development and Sustainability* 13, no. 3 (June 2011): 587–605. https://doi.org/10.1007/s10668-010-9278-0.

Koutsouris, Alexander J., Deliang Chen, and Steve W. Lyon. “Comparing Global Precipitation Data Sets in Eastern Africa: A Case Study of Kilombero Valley, Tanzania.” *International Journal of Climatology* 36, no. 4 (n.d.): 2000–2014. https://doi.org/10.1002/joc.4476.

Liebmann, Brant, Suzana J. Camargo, Anji Seth, José A. Marengo, Leila M. V. Carvalho, Dave Allured, Rong Fu, and Carolina S. Vera. “Onset and End of the Rainy Season in South America in Observations and the ECHAM 4.5 Atmospheric General Circulation Model.” *Journal of Climate* 20, no. 10 (May 1, 2007): 2037–50. https://doi.org/10.1175/JCLI4122.1.

Madi, Mohamed T., and Mohammad Z. Raqab. “Bayesian Prediction of Rainfall Records Using the Generalized Exponential Distribution.” *Environmetrics* 18, no. 5 (January 18, 2007): 541–49. https://doi.org/10.1002/env.826.

Maidment, Ross I., Richard P. Allan, and Emily Black. “Recent Observed and Simulated Changes in Precipitation over Africa: RECENT PRECIPITATION CHANGES OVER AFRICA.” *Geophysical Research Letters* 42, no. 19 (October 16, 2015): 8155–64. https://doi.org/10.1002/2015GL065765.

Mills, G. Fernandez. “Principal Component Analysis of Precipitation and Rainfall Regionalization in Spain.” *Theoretical and Applied Climatology* 50, no. 3–4 (1995): 169–83. https://doi.org/10.1007/BF00866115.

Mugume, Isaac, Charles Basalirwa, Daniel Waiswa, and Triphonia Ngailo. “Spatial Variation of WRF Model Rainfall Prediction over Uganda” 11, no. 7 (2017): 6.

National Research Council. *Lost Crops of Africa: Volume I: Grains*. Washington, D.C.: National Academies Press, 1996. https://doi.org/10.17226/2305.

Nicholson, Sharon E. “Climate and climatic variability of rainfall over eastern Africa.” *Reviews of Geophysics* 55, no. 3 (n.d.): 590–635. https://doi.org/10.1002/2016RG000544.

———. “The ITCZ and the Seasonal Cycle over Equatorial Africa.” *Bulletin of the American Meteorological Society* 99, no. 2 (February 2018): 337–48. https://doi.org/10.1175/BAMS-D-16-0287.1.

———. “The Nature of Rainfall Variability over Africa on Time Scales of Decades to Millenia.” *Global and Planetary Change* 26, no. 1 (2000): 137–158. https://doi.org/10.1016/S0921-8181(00)00040-0.

Nicholson, Sharon E., and Amin K. Dezfuli. “The Relationship of Rainfall Variability in Western Equatorial Africa to the Tropical Oceans and Atmospheric Circulation. Part I: The Boreal Spring.” *Journal of Climate; Boston* 26, no. 1 (January 1, 2013): 45–65.

Nicholson, Sharon E., Amin K. Dezfuli, and Douglas Klotter. "A Two-Century Precipitation Dataset for the Continent of Africa." *Bulletin of the American Meteorological Society* 93, no. 8 (August 2012): 1219–31. https://doi.org/10.1175/BAMS-D-11-00212.1.

Nicholson, Sharon E., and Jeeyoung Kim. "The Relationship of the El Niño–Southern Oscillation to African Rainfall." *International Journal of Climatology* 17, no. 2 (February 1, 1997): 117–35. https://doi.org/10.1002/(SICI)1097-0088(199702)17:2<117::AID-JOC84>3.0.CO;2-O.

Ouma, Jully O., Luke O. Olang, Gilbert O. Ouma, Christopher Oludhe, Laban Ogallo, and Guleid Artan. "Magnitudes of Climate Variability and Changes over the Arid and Semi-Arid Lands of Kenya between 1961 and 2013 Period." *American Journal of Climate Change* 07, no. 01 (January 17, 2018): 27. https://doi.org/10.4236/ajcc.2018.71004.

Pereira, Laura. "Climate Change Impacts on Agriculture across Africa." In *Oxford Research Encyclopedia of Environmental Science*, by Laura Pereira. Oxford University Press, 2017. https://doi.org/10.1093/acrefore/9780199389414.013.292.

Peterson, Thomas C., and David R. Easterling. "Creation of Homogeneous Composite Climatological Reference Series." *International Journal of Climatology* 14, no. 6 (n.d.): 671–79. https://doi.org/10.1002/joc.3370140606.

Peterson, Thomas C., and Russell S. Vose. "An Overview of the Global Historical Climatology Network Temperature Database." *Bulletin of the American Meteorological Society* 78, no. 12 (December 1997): 2837–49. https://doi.org/10.1175/1520-0477(1997)078<2837:AOOTGH>2.0.CO;2.

Peterson, Thomas C., Russell Vose, Richard Schmoyer, and Vyachevslav Razuvaëv. "Global Historical Climatology Network (GHCN) Quality Control of Monthly Temperature Data." *International Journal of Climatology* 18, no. 11 (n.d.): 1169–79. https://doi.org/10.1002/(SICI)1097-0088(199809)18:11<1169::AID-JOC309>3.0.CO;2-U.

Putnam, Aaron E., and Wallace S. Broecker. "Human-Induced Changes in the Distribution of Rainfall." *Science Advances* 3, no. 5 (May 31, 2017). https://doi.org/10.1126/sciadv.1600871.

Ropelewski, C. F., and M. S. Halpert. "Global and Regional Scale Precipitation Patterns Associated with the El Niño/Southern Oscillation." *Monthly Weather Review* 115, no. 8 (August 1, 1987): 1606–26. https://doi.org/10.1175/1520-0493(1987)115<1606:GARSPP>2.0.CO;2.

Schewe, Jacob, and Anders Levermann. "Non-Linear Intensification of Sahel Rainfall as a Possible Dynamic Response to Future Warming." *Earth System Dynamics* 8, no. 3 (July 5, 2017): 495–505. https://doi.org/10.5194/esd-8-495-2017.

Schneider, Tapio, Tobias Bischoff, and Gerald H. Haug. “Migrations and Dynamics of the Intertropical Convergence Zone.” *Nature; London* 513, no. 7516 (September 4, 2014): 45–53.

Schreck, Carl J., and Fredrick H. M. Semazzi. “Variability of the Recent Climate of Eastern Africa.” *International Journal of Climatology* 24, no. 6 (n.d.): 681–701. https://doi.org/10.1002/joc.1019.

Seregina, Larisa S., Andreas H. Fink, Roderick van der Linden, Nadir A. Elagib, and Joaquim G. Pinto. “A New and Flexible Rainy Season Definition: Validation for the Greater Horn of Africa and Application to Rainfall Trends.” *International Journal of Climatology* 39, no. 2 (February 1, 2019): 989–1012. https://doi.org/10.1002/joc.5856.

Si, Dong, YiHui Ding, and YanJu Liu. “Decadal Northward Shift of the Meiyu Belt and the Possible Cause.” *Chinese Science Bulletin* 54, no. 24 (December 1, 2009): 4742–48. https://doi.org/10.1007/s11434-009-0385-y.

Sylla, Mouhamadou, Michel Nikiema, Peter Gibba, Ibourahima Kebe, and Nana Ama Browne Klutse. “Climate Change over West Africa: Recent Trends and Future Projections,” 25–40, 2016. https://doi.org/10.1007/978-3-319-31499-0_3.

Thomas, Natalie, and Sumant Nigam. “Twentieth-Century Climate Change over Africa: Seasonal Hydroclimate Trends and Sahara Desert Expansion.” *Journal of Climate* 31, no. 9 (May 2018): 3349–70. https://doi.org/10.1175/JCLI-D-17-0187.1.

Tierney, J. E., J. M. Russell, Y. Huang, J. S. S. Damste, E. C. Hopmans, and A. S. Cohen. “Northern Hemisphere Controls on Tropical Southeast African Climate During the Past 60,000 Years.” *Science* 322, no. 5899 (October 10, 2008): 252–55. https://doi.org/10.1126/science.1160485.

Tierney, Jessica E., and Peter B. deMenocal. “Abrupt Shifts in Horn of Africa Hydroclimate Since the Last Glacial Maximum.” *Science* 342, no. 6160 (November 15, 2013): 843–46. https://doi.org/10.1126/science.1240411.

Tierney, Jessica E., Peter B. deMenocal, and Paul D. Zander. “A Climatic Context for the Out-of-Africa Migration.” *Geology* 45, no. 11 (November 1, 2017): 1023–26. https://doi.org/10.1130/G39457.1.

Tierney, Jessica E., Jason E. Smerdon, Kevin J. Anchukaitis, and Richard Seager. “Multidecadal Variability in East African Hydroclimate Controlled by the Indian Ocean.” *Nature* 493, no. 7432 (January 16, 2013): 389–92. https://doi.org/10.1038/nature11785.

Tierney, Jessica E., Caroline C. Ummenhofer, and Peter B. deMenocal. “Past and Future Rainfall in the Horn of Africa.” *Science Advances* 1, no. 9 (October 9, 2015). https://doi.org/10.1126/sciadv.1500682.

Tropical Rainfall Measuring Mission (TRMM) (2011), TRMM (TMPA/3B43) Rainfall Estimate L3 1 month 0.25 degree x 0.25 degree V7, Greenbelt, MD, Goddard Earth Sciences Data and Information Services Center (GES DISC), Accessed: February 2nd, 2019, 10.5067/TRMM/TMPA/MONTH/7

Yang, Wenchang, Richard Seager, Mark A. Cane, and Bradfield Lyon. “The Annual Cycle of East African Precipitation.” *Journal of Climate* 28, no. 6 (March 2015): 2385–2404. https://doi.org/10.1175/JCLI-D-14-00484.1.

Appendix A

Regional correlations between the first five principal components of each seasonal parameter and four well-known climate indices—Niño 3.4, the North Atlantic Oscillation (NAO), the Atlantic Meridional Mode (AMM), and the Indian Ocean dipole (IOD)— for each of the 10 studied clusters are presented below. The two highest correlations exceeding an absolute value of 0.1 for each region are highlighted in color.

***

Timing is most strongly correlated:

In *Region 1* with Niño 3.4, the NAO and the AMM, all in the 4th component.

In *Region 2* with Niño 3.4 and the NAO in the 2nd and 5th components. Less strongly correlated with the AMM in the 1st and 4th components.

In *Region 3* with the IOD in the 1st and 4th components and with the AMM in the 1st and 2nd components.

In *Region 4* with the IOD in the 1st and 3rd components.

In *Region 5* with AMM in the 4th and 5th components and with IOD in the 5th component.

In *Region 6* with the AMM in the 4th and 5th components, Niño 3.4 and NAO in the 1st and 3rd components, and the IOD in the 2nd and 5th components.

In *Region 7* with the AMM in the 1st and 2nd components, and with Niño 3.4 and the NAO in the 1st and 4th components

In *Region 8* with Niño 3.4 and the NAO in the 3rd and 5th components.

In *Region 9* with each climate index, though Niño 3.4 and NAO manifest in the 1st and 2nd components, IOD in the 1st and 3rd, and AMM in the 1st and 4th.

In *Region 10* with the AMM in the 1st component.

	Regional Timing				
	1st	2nd	3rd	4th	5th
	El Niño				
1	-0.12	0.13	0.10	-0.29	0.11
2	-0.15	0.31	-0.15	-0.16	0.32
3	-0.04	-0.18	0.05	-0.03	0.20
4	0.06	0.23	0.16	-0.16	0.19
5	-0.17	0.07	-0.12	-0.06	0.01
6	-0.48	0.03	0.26	0.03	-0.02
7	0.30	0.00	-0.04	0.33	0.11
8	-0.18	0.17	0.25	-0.03	-0.44
9	-0.24	-0.19	0.11	-0.13	0.00
10	0.23	0.12	0.16	-0.27	-0.32
	North Atlantic Oscillation				
1	-0.11	0.13	0.10	-0.30	0.10
2	-0.14	0.30	-0.15	-0.15	0.31
3	-0.05	-0.18	0.04	-0.03	0.19
4	0.06	0.23	0.16	-0.16	0.20
5	-0.17	0.08	-0.11	-0.06	0.01
6	-0.48	0.03	0.26	0.03	-0.02
7	0.31	0.00	-0.05	0.33	0.11
8	-0.18	0.17	0.25	-0.03	-0.44
9	-0.24	-0.19	0.11	-0.13	0.00
10	0.23	0.12	0.15	-0.27	-0.32
	Indian Ocean Dipole				
1	0.02	0.11	0.16	0.01	-0.12
2	0.08	-0.04	-0.10	0.18	0.02
3	0.27	-0.15	0.11	-0.37	-0.01
4	-0.35	-0.03	-0.24	0.09	0.08
5	0.04	0.20	-0.03	-0.17	-0.32
6	0.10	0.02	0.10	-0.03	-0.36
7	0.12	0.21	0.05	0.32	0.02
8	0.21	0.05	0.21	0.16	0.00
9	0.24	0.02	0.11	-0.01	0.09
10	0.23	-0.27	-0.08	0.28	0.09
	Atlantic Meridional Mode				
1	0.12	0.12	0.04	0.32	0.20
2	-0.24	0.03	0.20	-0.21	0.04
3	-0.21	0.37	0.06	0.00	0.18
4	0.11	-0.09	0.06	-0.05	-0.11
5	-0.13	-0.05	-0.21	0.36	0.30
6	0.16	0.04	0.09	0.35	0.37
7	-0.41	-0.25	0.00	-0.14	-0.20
8	-0.15	0.06	-0.04	0.06	0.24
9	-0.27	0.02	0.03	-0.14	-0.05
10	-0.40	0.01	0.07	0.08	-0.04

Table 1: Correlations of the first five principal components of each regional seasonal timing timeseries with four common climate indices. The two highest values for each region are highlighted in color; Niño 3.4 in green, the North Atlantic Oscillation in yellow, the Indian Ocean Dipole in blue, and the Atlantic Meridional Mode in red.

Magnitude is most strongly correlated:

In *Region 1* with the AMM in the 1st component.

In *Region 2* with the AMM in the 4th and 5th components.

In *Region 3* with the AMM in the 2nd and 3rd components.

In *Region 4* with the AMM in the 1st and 5th components.

In *Region 5* with Niño 3.4 and NAO in the 4th and 5th components and with IOD in the 3rd and 4th components.

In *Region 6* with the AMM in the 1st and 3rd components.

In *Region 7* with the IOD in the 4th component.

In *Region 8* with the AMM in the 1st and 3rd components.

In *Region 9* with the AMM in the 3rd component.

In *Region 10* with the AMM also in the 3rd component.

***

Duration is most strongly correlated:

In *Region 1* with Niño 3.4 and NAO in the 2nd and 4th components.

In *Region 2* with the AMM in the 1st and 5th components.

In *Region 3* with the AMM in the 5th component.

In *Region 4* with Niño 3.4 and NAO in the 2nd component.

In *Region 5* with AMM in the 2nd and 5th components.

In *Region 6* with the AMM in the 1st and 4th components.

In *Region 7* with the AMM in the 3rd component.

In *Region 8* with the AMM in the 2nd component.

In *Region 9* with Niño 3.4 and NAO in the 1st and 5th components.

In *Region 10* with Niño 3.4 and NAO in the 1st and 2nd components.

	Regional Magnitude				
	1st	2nd	3rd	4th	5th
	El Niño				
1	-0.08	-0.13	-0.07	0.22	-0.12
2	0.11	0.03	0.11	0.08	0.18
3	0.09	-0.16	0.04	-0.17	-0.08
4	-0.11	0.03	-0.02	0.17	0.03
5	0.07	-0.11	-0.06	-0.31	0.12
6	0.28	-0.13	0.12	-0.08	0.13
7	0.27	-0.28	-0.29	0.05	-0.26
8	0.03	0.01	-0.12	0.10	0.05
9	0.16	-0.07	-0.15	0.14	-0.05
10	0.28	0.00	0.08	-0.12	0.18
	North Atlantic Oscillation				
1	-0.08	-0.13	-0.06	0.21	-0.12
2	0.11	0.03	0.11	0.08	0.18
3	0.09	-0.16	0.04	-0.17	-0.08
4	-0.12	0.04	-0.02	0.17	0.03
5	0.07	-0.12	-0.05	-0.31	0.12
6	0.28	-0.12	0.11	-0.08	0.13
7	0.27	-0.27	-0.29	0.04	-0.27
8	0.04	0.01	-0.12	0.10	0.05
9	0.16	-0.07	-0.15	0.13	-0.05
10	0.28	0.01	0.08	-0.13	0.18
	Indian Ocean Dipole				
1	-0.28	0.10	-0.19	0.13	-0.11
2	-0.04	-0.05	0.01	0.13	0.13
3	0.23	-0.11	-0.05	-0.21	0.04
4	-0.10	-0.25	-0.16	0.05	-0.05
5	0.01	-0.04	-0.32	-0.13	-0.09
6	-0.09	-0.09	0.05	-0.16	0.08
7	-0.12	0.19	-0.27	0.40	0.12
8	-0.03	-0.29	-0.02	0.03	-0.02
9	-0.09	-0.09	-0.07	0.02	0.12
10	-0.17	-0.25	-0.02	-0.08	0.21
	Atlantic Meridional Mode				
1	0.57	-0.17	-0.08	-0.10	-0.01
2	0.14	-0.01	-0.19	0.29	-0.38
3	0.01	0.22	0.33	0.06	0.16
4	0.33	-0.05	0.08	-0.12	0.14
5	0.23	0.27	0.12	0.03	-0.03
6	0.25	0.11	0.27	0.14	-0.01
7	0.34	0.01	0.28	0.05	0.00
8	0.16	0.00	-0.37	0.03	0.09
9	0.15	-0.13	0.32	0.12	0.03
10	0.23	0.28	-0.43	0.31	-0.23

Table 2: same as Table 1, but for seasonal magnitude.

	Regional Duration				
	1st	2nd	3rd	4th	5th
	El Niño				
1	-0.19	0.26	-0.11	0.36	0.08
2	0.22	0.08	-0.19	-0.04	0.09
3	0.12	0.00	-0.20	0.13	0.06
4	0.22	-0.48	0.09	0.01	0.02
5	-0.06	-0.09	0.34	-0.08	-0.18
6	-0.32	-0.04	-0.22	-0.05	0.14
7	0.27	0.37	0.17	-0.37	0.15
8	0.17	0.14	-0.09	-0.19	0.06
9	0.30	0.15	-0.04	0.02	-0.38
10	0.45	-0.41	0.08	-0.09	-0.10
	North Atlantic Oscillation				
1	-0.19	0.27	-0.11	0.35	0.08
2	0.22	0.08	-0.19	-0.04	0.09
3	0.11	0.01	-0.21	0.13	0.06
4	0.21	-0.48	0.09	0.01	0.03
5	-0.05	-0.08	0.34	-0.08	-0.17
6	-0.32	-0.04	-0.22	-0.06	0.14
7	0.27	0.37	0.16	-0.37	0.15
8	0.17	0.14	-0.09	-0.18	0.07
9	0.31	0.15	-0.04	0.02	-0.38
10	0.45	-0.41	0.08	-0.09	-0.11
	Indian Ocean Dipole				
1	-0.04	0.23	0.02	-0.07	-0.11
2	0.17	-0.16	-0.04	0.10	0.36
3	0.08	0.27	0.13	0.20	-0.26
4	0.07	-0.04	-0.23	0.06	-0.04
5	0.15	-0.17	-0.04	0.14	0.16
6	-0.17	-0.02	-0.29	-0.13	-0.18
7	0.25	0.11	-0.39	-0.11	-0.01
8	-0.06	-0.21	-0.21	-0.16	0.03
9	-0.07	0.09	0.02	0.09	-0.05
10	-0.08	0.01	0.14	0.14	-0.27
	Atlantic Meridional Mode				
1	0.22	-0.30	0.07	0.13	0.02
2	-0.34	-0.08	0.13	-0.13	-0.42
3	0.02	-0.05	0.13	-0.19	0.31
4	-0.12	0.00	0.25	0.04	-0.07
5	0.07	-0.36	0.03	-0.22	-0.39
6	0.38	-0.19	0.26	0.33	0.08
7	-0.39	-0.23	0.61	0.08	-0.19
8	-0.14	0.40	0.06	0.03	-0.17
9	-0.20	-0.04	-0.28	-0.13	-0.13
10	0.15	0.21	-0.30	-0.31	0.27

Table 3: same as Table 1, but for seasonal duration.

Appendix B

We have chosen to represent the location of the ITCZ over the course of this study using measurements of seasonal timing produced by our proposed mixed Gaussian model. To isolate trends in the timing of the ITCZ's equatorial crossing, we transformed a geographic map into a temporal map of sorts, according the process outlined in Figure 27.

In step **(i)**, we plotted the month of seasonal timing across a gridded version of the GHCN and TRMM data networks used in the previous analyses. This was done for both boreal spring and fall, though for the purposes of illustration, only the boreal spring for 1936 is shown in Figure 27. We then averaged those values across all longitudes in every year (step **(ii)**), creating a single annual column of zonally averaged seasonal timing. Next, we created a p-color chart by plotting all years next to one another in step **(iii)**, which illustrated zonally averaged change over time. Finally, we isolated the zonal values for each year at 0^{o} N, which correspond with the timing of peak rainfall in each season at the equator. The trends in those values, shown in step **(iv)**, imply the shift in the ITCZ's average position outlined previously.

While this method can really only address continent-scale change, we find it appropriate to use when tracking a system as large as the ITCZ.

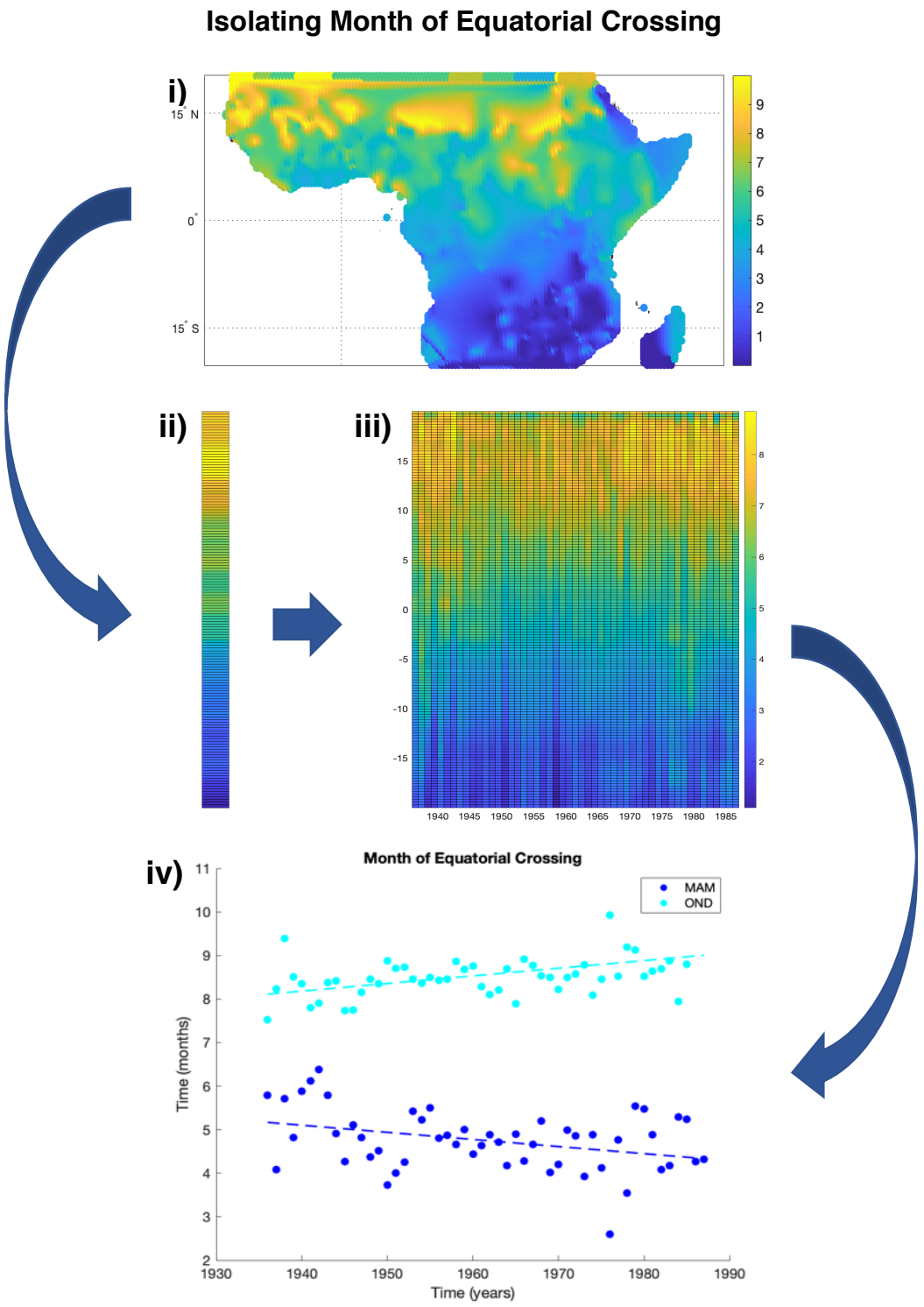

Figure 27: Schematic for the process of isolating the month of the rain belt's equatorial crossing for the boreal spring (dark blue) and boreal fall (cyan) rainy seasons. Steps include: **i)** a gridded map of seasonal timing for the boreal spring in a given year; **ii)** a column representing one year of zonally averaged seasonal timing; **iii)** the 'temporal map' composite of every year from **(ii)**; **iv)** the trends of values isolated along the equator.